U.S. Department of
Transportation
**Federal Railroad
Administration**

Rail Base Corrosion and Cracking Prevention

Office of Research
and Development
Washington, DC 20590

DOT/FRA/ORD-14/27

Final Report
July 2014

REPORT DOCUMENTATION PAGE

Form Approved
OMB No. 0704-0188

1. AGENCY USE ONLY (Leave blank)	2. REPORT DATE	3. REPORT TYPE AND DATES COVERED
	July 2014	Final (September 2012 – June 2013)

4. TITLE AND SUBTITLE
Rail Base Corrosion and Cracking Prevention

5. FUNDING NUMBERS
DTFR-12-C-0024

6. AUTHOR(S)
Dr. George W. Ritter, EWI; Dr. William C. Mohr, EWI; Dr. David Y. Jeong, Volpe NTS Center; Yim A. Tang, Volpe NTS Center; Cameron Stuart, Federal Railroad Administration, US DOT

7. PERFORMING ORGANIZATION NAME(S) AND ADDRESS(ES)
EWI
1250 Arthur E. Adams Drive
Columbus, OH 43221

8. PERFORMING ORGANIZATION REPORT NUMBER
EWI Project No. 53331GTH (Rev. 2)

9. SPONSORING/MONITORING AGENCY NAME(S) AND ADDRESS(ES)
U.S. Department of Transportation
Federal Railroad Administration
Office of Research and Development
Washington, DC 20590

10. SPONSORING/MONITORING AGENCY REPORT NUMBER
DOT/FRA/ORD-14/27

11. SUPPLEMENTARY NOTES
COTR: Cameron D. Stuart

12a. DISTRIBUTION/AVAILABILITY STATEMENT
This document is available to the public through the FRA Web site at http://www.fra.dot.gov or by calling (202) 493-1300.

12b. DISTRIBUTION CODE

13. ABSTRACT (Maximum 200 words)
Rail base corrosion combined with fatigue or damage can significantly reduce rail life. Studies were done to examine the relative contribution of damage, corrosion, and fatigue on rail life. The combined effects can be separated into constituent factors. Anti-corrosion treatments based on surface passivation of steel have been shown to extend rail fatigue life in the presence of damage and corrosion.

14. SUBJECT TERMS
Rail base corrosion, corrosion, corrosion treatments, fatigue, rail life

15. NUMBER OF PAGES
60

16. PRICE CODE

17. SECURITY CLASSIFICATION OF REPORT	18. SECURITY CLASSIFICATION OF THIS PAGE	19. SECURITY CLASSIFICATION OF ABSTRACT	20. LIMITATION OF ABSTRACT
Unclassified	Unclassified	Unclassified	SAR

NSN 7540-01-280-5500
Standard Form 298 (Rev. 2-89)
Prescribed by ANSI Std. 239-18
298-102

METRIC/ENGLISH CONVERSION FACTORS

ENGLISH TO METRIC	METRIC TO ENGLISH
LENGTH (APPROXIMATE)	**LENGTH (APPROXIMATE)**
1 inch (in) = 2.5 centimeters (cm)	1 millimeter (mm) = 0.04 inch (in)
1 foot (ft) = 30 centimeters (cm)	1 centimeter (cm) = 0.4 inch (in)
1 yard (yd) = 0.9 meter (m)	1 meter (m) = 3.3 feet (ft)
1 mile (mi) = 1.6 kilometers (km)	1 meter (m) = 1.1 yards (yd)
	1 kilometer (km) = 0.6 mile (mi)
AREA (APPROXIMATE)	**AREA (APPROXIMATE)**
1 square inch (sq in, in^2) = 6.5 square centimeters (cm^2)	1 square centimeter (cm^2) = 0.16 square inch (sq in, in^2)
1 square foot (sq ft, ft^2) = 0.09 square meter (m^2)	1 square meter (m^2) = 1.2 square yards (sq yd, yd^2)
1 square yard (sq yd, yd^2) = 0.8 square meter (m^2)	1 square kilometer (km^2) = 0.4 square mile (sq mi, mi^2)
1 square mile (sq mi, mi^2) = 2.6 square kilometers (km^2)	10,000 square meters (m^2) = 1 hectare (ha) = 2.5 acres
1 acre = 0.4 hectare (he) = 4,000 square meters (m^2)	
MASS - WEIGHT (APPROXIMATE)	**MASS - WEIGHT (APPROXIMATE)**
1 ounce (oz) = 28 grams (gm)	1 gram (gm) = 0.036 ounce (oz)
1 pound (lb) = 0.45 kilogram (kg)	1 kilogram (kg) = 2.2 pounds (lb)
1 short ton = 2,000 pounds (lb) = 0.9 tonne (t)	1 tonne (t) = 1,000 kilograms (kg)
	= 1.1 short tons
VOLUME (APPROXIMATE)	**VOLUME (APPROXIMATE)**
1 teaspoon (tsp) = 5 milliliters (ml)	1 milliliter (ml) = 0.03 fluid ounce (fl oz)
1 tablespoon (tbsp) = 15 milliliters (ml)	1 liter (l) = 2.1 pints (pt)
1 fluid ounce (fl oz) = 30 milliliters (ml)	1 liter (l) = 1.06 quarts (qt)
1 cup (c) = 0.24 liter (l)	1 liter (l) = 0.26 gallon (gal)
1 pint (pt) = 0.47 liter (l)	
1 quart (qt) = 0.96 liter (l)	
1 gallon (gal) = 3.8 liters (l)	
1 cubic foot (cu ft, ft^3) = 0.03 cubic meter (m^3)	1 cubic meter (m^3) = 36 cubic feet (cu ft, ft^3)
1 cubic yard (cu yd, yd^3) = 0.76 cubic meter (m^3)	1 cubic meter (m^3) = 1.3 cubic yards (cu yd, yd^3)
TEMPERATURE (EXACT)	**TEMPERATURE (EXACT)**
[(x-32)(5/9)] [= y □C	[(9/5) y + 32] | = x □F

QUICK INCH - CENTIMETER LENGTH CONVERSION

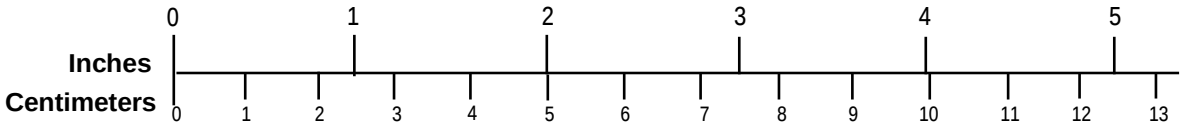

QUICK FAHRENHEIT - CELSIUS TEMPERATURE CONVERSIO

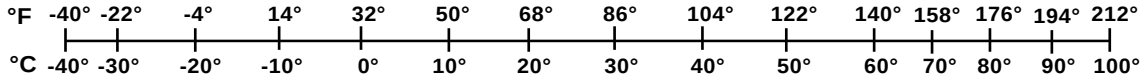

For more exact and or other conversion factors, see NIST Miscellaneous Publication 286, Units of Weights and Measures. Price $2.50 SD Catalog No. C13 10286

Updated 6/17/98

Contents

Illustrations

Tables

Executive Summary

Rail base corrosion can take place when water gets trapped between the flange base and the tie plate. Corrosion is accelerated by the presence of salt in the water and electrical current transmitted through the rail base and the tie plate path to earth ground. This corrosion results in the loss of rail base material and strength. Ultimately, it is possible for the rail to fail. Rail base corrosion has been suspected as a cause for derailments in the recent past. This program was initiated to examine treatment methods to prevent or forestall rail base corrosion. The program was funded by the Federal Railroad Administration (FRA) and executed by Edison Welding Institute (EWI).

The most obvious way to protect steel against corrosion is to paint it with a barrier-type coating. Barrier-type coatings, like paint, have a limited life due to loss of adhesion and/or abrasive wear. Another approach is to treat the rail surface chemically to passivate (protect) the surface against rusting or slow the progress of rusting substantially. This was the overall approach used in this work.

Rail is subjected to fatigue loads in normal service. These loads can lead to small cracks in the rail. When corrosion forms in these cracks, the rail loses significant strength. For this program, the combined effects of damage, corrosion, and fatigue were examined under controlled conditions to ascertain the relative contribution of each to the overall condition of the rail and to measure the performance of anti-corrosion treatments in limiting corrosion and extending the rail's fatigue life.

An organometallic conversion type coating system, investigated at EWI for use in high pressure liquid water systems, was useful in retarding the effects of corrosion on fatigue rail life. However, it did not prevent corrosion in the presence of saltwater or condensing humidity. A commercially available inorganic conversion coating (EonCoat®) was effective in preventing corrosion in saltwater environments. It enabled extended fatigue life, even on damaged rail subjected to aggressive corrosive environments, and gave performance similar to that for undamaged, uncorroded rail.

In this work, it was found that the interactions between rail damage, corrosive attack, and overall rail fatigue life can be examined by methodical application of traditional four-point fatigue testing using manageable sample sizes. The influences of corrosion and damage in the presence of fatigue stress are believed to be separable based on this limited testing. The presence of damage alone showed reduced rail fatigue life by as much as one order of magnitude. Rail fatigue life is reduced by as much as an additional order of magnitude when these damaged areas are corroded. The combined effects on rail life of damage, corrosion, and fatigue can be severe. Use of corrosion protection systems, applied to the base of the rail flange, can extend rail fatigue life.

A resonant fatigue test method was adapted for use with 20-foot long rail segments. It was shown that asymmetrical and heavy cross sections could, in fact, be induced into self-oscillation, developing roughly 60–80 ksi peak stress. In this work, the method was not found to be predictive of fatigue life for damaged, corroded rail, with or without corrosion protection. However, rail was taken to failure by this method, suggesting that a more advanced test methodology might be useful for screening rail fatigue phenomena.

Based on the results of this preliminary work, the researchers recommend continued analysis of these corrosion inhibiting treatments. Field trails of these treatments to support the laboratory results is a necessary step towards in-service deployment.

1. Introduction

Rail base corrosion has been observed by several rail operators in tunnels where water is periodically present at the base of the rail. The Transit Cooperative Research Program/Transportation Technology Center, Inc. (TCRP/TTCI) review[1] of this behavior found that the most severe corrosion was reported in tunnels in the New York City area. Some corrosion was invasive and found to advance as much as one-fourth inch up from the area where the rail base crosses tie plates. References containing this information also warned of the possibility that the edge of the corroded area could act as a stress concentrator that would allow fatigue crack growth up the rail.[2,3] Further, the effects of corrosive antagonists can be amplified by mechanical abuse and fatigue, exposure to road deicing materials, and leakage currents for electrified rail. This program was initiated to investigate rail treatments that can mitigate the effects of humidity, saline exposure, and fatigue on crack growth in rail steels.

A recent failure in a tunnel in the New York City area was found to be a fatigue-type failure initiating from the rail base at the edge of the corroded area. Plans are underway for rail replacement in and beyond the area of the derailment. However, there is significant interest from operators such as Amtrak, Long Island Rail Road (LIRR), and Port Authority Trans-Hudson (PATH) in extending the life of rails in tunnels by minimizing or eliminating the issue of rail corrosion and associated fatigue cracking. Further, there are many areas throughout the country where similar corrosion, or corrosion caused by condensing or dripping water, occurs. Treatment of the rail bottom surface to limit the effect of corrosion mechanisms may help increase rail life, reliability, and overall rail safety.[4,5]

Reducing or mitigating rail corrosion speaks directly to safety in operations and reliability of infrastructure. The technology under study is expected to be applicable to new rail and possibly to installed rail as a remedial measure. It is believed that the treated rail can be installed following established procedures. It may also be beneficial to use treated rail and tie plates in combination on electrified rail lines. Potential users with tunnels in the New York City area (Amtrak, PATH, LIRR, etc.) have been made aware of this technology development by representatives from the Volpe National Transportation Systems Center (Volpe).

1.1 Background

Efforts to control corrosion on track segments are not new. Most approaches involve protecting the rail with paint-like materials or coatings. These materials provide a barrier to corrosive elements, but they do not prevent their ultimate intrusion. Wear resistance is also an important factor in the lifetime of protection. In this research program, EWI tested rail treatments that are designed to alter the surface chemistry of the rail such that it impedes or rejects corrosion. Two of the treatments were based on work previously done at EWI for corrosion protection in nuclear piping.[6] The third treatment is commercially available.[7]

When iron rusts, it oxidizes first to ferrous ion (Fe^{+2}). This process can be initiated by the influence of chloride salts found in road deicing mixtures. Further reactions between iron, oxygen, and water result in the formation of ferric ions (Fe^{+3}). All these species exist as oxides on the metal surface.

Interestingly, ferrous oxide (FeO – black rust) is rather stable in water, and the mixed oxide, Fe_3O_4, a mixture of FeO and Fe_2O_3, is also fairly stable. It is the red rust form, Fe_2O_3, that is commonly referred to as "rust" or "bleeding rust" – that is invasive and destructive of the iron underneath. If the surface oxides can be driven back to the more stable forms, such as FeO or Fe_3O_4 mixed oxide, "rusting" can be abated and controlled.

Corrosion prevention methods include creating a barrier (i.e. paint) to prevent corrosive elements from reaching the base metal, adding a sacrificial material to the steel (i.e., galvanizing), using electrical charge to reverse oxidation (cathodic protection), or using a chemical conversion to discourage the formation of ferric oxide rust. This research project examined surface conversion methods for rust mitigation or prevention.

1.2 Objectives

The primary objectives of this project were to:

1) Examine selected anti-corrosion treatments that render the rail surface immune to corrosion or mitigate its spread should initial corrosion occur.
2) Introduce elements of flexural fatigue to the rail to examine the combined effects of corrosion and fatigue in crack propagation.
3) Delineate, if possible, the relative contributions of damage, corrosion, and fatigue level to the reduction of rail fatigue life.
4) Examine the use of a resonant fatigue methodology for its applicability to rail, and specifically, as a predictive tool for this investigation. Compare this method with four-point load fatigue methods.

1.3 Technical Approach

A summarized Work Breakdown Structure is shown below.

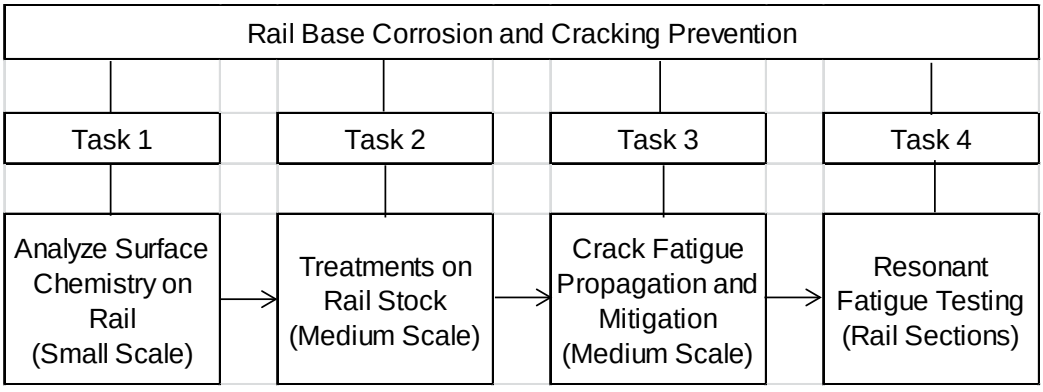

Figure 1. High-Level Work Breakdown Structure

2. Experimental Activities

2.1 Task 1 – Analyze Surface Chemistry on Rail (Small Scale)

Task 1 of this program examined protective treatments on small samples of rail steel and the effects of corrosive attack on surface chemistries. The objective was to document the effect of these treatments on rail steel and to determine if there was a need to heat-treat the ceramic precursor coating.

One-inch wide test specimens were cut from the web of standard 136-pound rail (common rail steel), degreased in an aqueous cleaner and wiped with isopropyl alcohol, and subsequently treated with EWI-developed combinations of phosphoric acid etch, an iron conversion coating, and a zirconium oxide sol-gel.[8] Following these varied treatments, some samples were subjected to 3 weeks of cyclic corrosion, while other similarly treated counterparts were kept aside as controls. Those exposed to corrosion were then examined visually for their general performance and also analyzed using scanning electron microscopy (SEM) and elemental x-ray dispersive analysis (EDS) to examine surface condition and chemistry.

They were then treated according to the outline presented in Table 1.

2.1.1 Sample Corrosion Exposures

Table 1. Sample Disposition for Treatments

Sample Preparation							
	No Induced Corrosion	Induced Corrosion	P	D	Z	Bake	Total
2-step	PD1	PD2	X	X			6
	PD3	PD4	X	X			
	PD5	PD6	X	X			
	PZ1	PZ2	X		X	X	2
3-step	PDZ1	PDZ2	X	X	X		6
	PDZ3	PDZ4	X	X	X		
	PDZ5	PDZ6	X	X	X		
	ALL1	ALL2	X	X	X	X	2

P = phosphoric acid; D = di=phenolic converting agent; Z = zirconium-oxide sol-gel sealer

The EWI system can be applied using two or three treatment steps, as described below. Their designations are:

1. PD (two-step) – Consists of a treatment with phosphoric acid (P), followed by treatment with a di-phenolic converting agent (D).

2. PZ (two-step) – Consists of a treatment with phosphoric acid, followed by application of a zirconium-oxide producing sol-gel sealer (Z), followed by a post bake at 550°C with a 3-hour hold at temperature.
3. PDZ (three-step, no post bake) – The PD process is followed by application of a zirconium-oxide producing sol-gel sealer. There is no post bake.
4. ALL (three-step, with post bake) – The PDZ process, followed by a post bake at 550°C with a 3-hour hold at temperature.

P, D, and Z may be applied sequentially by spray or brush.

All rail specimens were treated with a 10 percent phosphoric acid solution (P) (by weight in water). Grit-blasting was used to remove surface rust to get down to base metal.

Air drying following the phosphoric acid application produced a white, powdery material on the surface. The surface was then wiped with water to remove the excess crystal formation.

For the D treatment, the phosphated rail was treated with the di-phenolic reducing agent, also brush applied. A deep blue-black color emerged, indicating the formation of the mixed metal oxide of $FeO \cdot Fe_2O_3$. After drying for 4–6 hours, the sample was washed with water to remove excess reducing agent.

After the P and any applied D treatment, the Z step consisted of applying a zirconia sol-gel. A sol-gel is a ceramic precursor solution derived from an organometallic precursor in alcohol solvent. The precursor hydrolyzes to form an oxy-hydroxide zirconate that can be heated to form zirconium oxide ceramic. The preparation of this material was taken from the literature.[8] Heating the coated rail to a temperature of 550°C for 3 hours converted the sol-gel to a form of zirconium oxide. This temperature is well below the transition temperature between ferrite and austenite for common rail steels (~700°C), thus avoiding martensite formation upon cooling. The hardness of these treated steels never dropped below 325 Brinell.

The three-step process (ALL) used a muffle furnace for the bake step. There were two two-step variants. One involved using only the phosphate and the di-phenol, with no zirconia seal or bake (PD). The other used the phosphate treat and zirconia seal with a bake (PZ).

The bake for PZ1, PZ2, ALL1, and ALL2 specimens consisted of heating them in air at 550°C for 3 hours to set the zirconia ceramic seal coat. (Testing showed that this heat soak cycle of rail steel in air gave a Brinell hardness of 329.) PZ1 and PZ2 were not treated with the iron conversion coating, but were baked to produce possible iron-zirconium phosphate complexes. ALL1 and ALL2 were also baked.

The "even numbered" specimens were subjected to a 3-week cycle of corrosion, while the "odd numbered" specimens were set aside as controls. The corrosion cycle is given in Table 2. The saline solution was made up of a 5 percent by weight addition of road deicing salt in tap water. Road deicing salt also contains calcium chloride and magnesium salts in addition to the predominant sodium chloride (rock salt). The hot and wet conditions were 50°C with 98–100 percent relative humidity in a closed-temperature humidity chamber. This type of corrosion cycle was designed to be exceptionally severe compared with normal operating conditions for rail, so that differences in corrosion protection or attack could be shown rapidly.

Table 2. Corrosion Cycles for Even-Numbered Specimens

Corrosion Cycles							
Week 1	Tues	Weds	Thurs*	Fri	Sat	Sun	Mon*
Day	1	2	3	4	5	6	7
Exposure	Salt water	Salt water	Dry (out)	Humidity	Humidity	Humidity	Dry (out)
Week 2	Tues	Weds	Thurs*	Fri	Sat	Sun	Mon*
Day	8	9	10	11	12	13	14
Exposure	Salt water	Salt water	Dry (out)	Humidity	Humidity	Humidity	Dry (out)
Week 3	Tues	Weds	Thurs*	Fri	Sat	Sun	Mon*
Day	15	16	17	18	19	20	21
Exposure	Salt water	Salt water	Dry (out)	Humidity	Humidity	Humidity	Dry (out)
	* Samples removed and pictures taken						

2.1.2 SEM and EDS Analyses

Sample bars representing the different treatments and corrosion exposure histories were taken from the series and examined with a Zeiss EVO Model 60 scanning electron microscope equipped with an Oxford Instruments X-Max Energy Dispersive Spectroscopy (EDS) for elemental analysis. The sample selection was based on visual appearance and apparent resistance to corrosion attack.

2.2 Task 2 – Treatments on Rail Stock (Medium-Scale) and Tie Plates

Treatments that showed the best corrosion resistance in Task 1 were selected for further study in Task 2 and Task 3 of the program. In Task 2, larger rail segments (~6- × 18-in. segments of flange bases) were notched (Figure 2), treated, and exposed for a period of 3 weeks to an aggressive corrosive environment consisting of a saltwater soak and condensing humidity.

Based on the results from Task 1, the PD two-step variant and the ALL system three-step variant were selected to be treated in Task 2 and tested in Task 3. EonCoat®, a commercially-available material, was also tested.

EonCoat® is a commercially spray-applied ceramic coating.[7] The overall formulation is proprietary. It is applied using standard two-component spray equipment with a mixer-head nozzle. It dries within minutes of application. A second coat can be applied in approximately 10–15 minutes, which was the practice used here. EonCoat® was applied by the vendor, and the plate sets were returned to EWI.

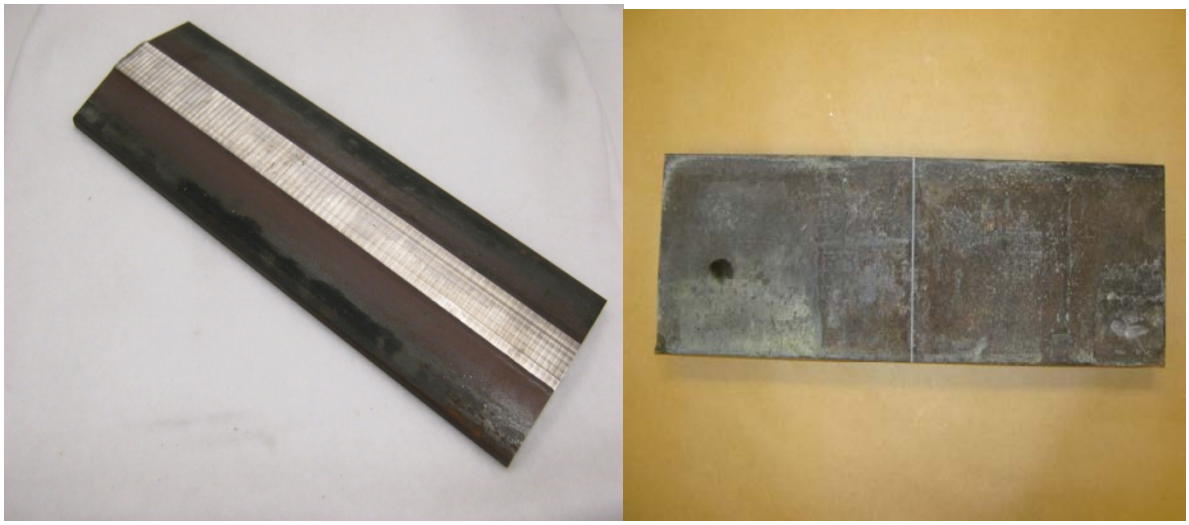

Figure 2. Flange Detail Showing Bottom Cut Notch (Right)

Six specimens were tested:

1. Undamaged rail, no protection, no corrosion (control using just a flange base);
2. Untreated rail, damaged (notched), but with no corrosion. This represents a baseline field installation that has been in use but is not in a corrosive environment ordinarily;
3. Untreated rail, notched, with corrosion exposure. This was resting on an untreated tie plate throughout the corrosion cycling. This represents the baseline field installation in a corrosive environment, such as a rail tunnel or drip zone;
4. The three-step treated rail section (ALL), notched, with corrosion exposure. This was resting on an ALL-treated tie plate throughout the corrosion cycling. This shows the effect of trapped corrosive elements between the bottom of the rail and the tie plate having protection by the ALL method;
5. The two-step treated rail section (DP), notched, with corrosion exposure. This was resting on a DP-treated tie plate throughout the corrosion exposure. This shows the effect of trapped corrosive elements between the bottom of the rail and the tie plate having protection by the DP method; and
6. An EonCoat® treated rail section, notched, with corrosion exposure. This was resting on an EonCoat® treated tie plate throughout the corrosion exposure. This shows the effect of trapped corrosive elements between the bottom of the rail and the tie plate having protection by the EonCoat® material.

Notching, if used, was done *before* any treatments were applied and/or before corrosion exposure.

2.2.1 Preparation and Treatment of Medium-Scale Specimens

All the flange pieces and tie plates were grit-blasted to remove excess scale and rust. The appropriate treatments were then applied using the same approaches as those for Task 1. The ALL three-step samples were baked at 550°C for 3 hours to set the zirconium oxide sol-gel sealer. The samples, as placed into the bake furnace, are shown in Figure 3, and the thermocouple trace for the bake is shown in Figure 4.

Figure 3. (ALL) Specimens in Bake Furnace

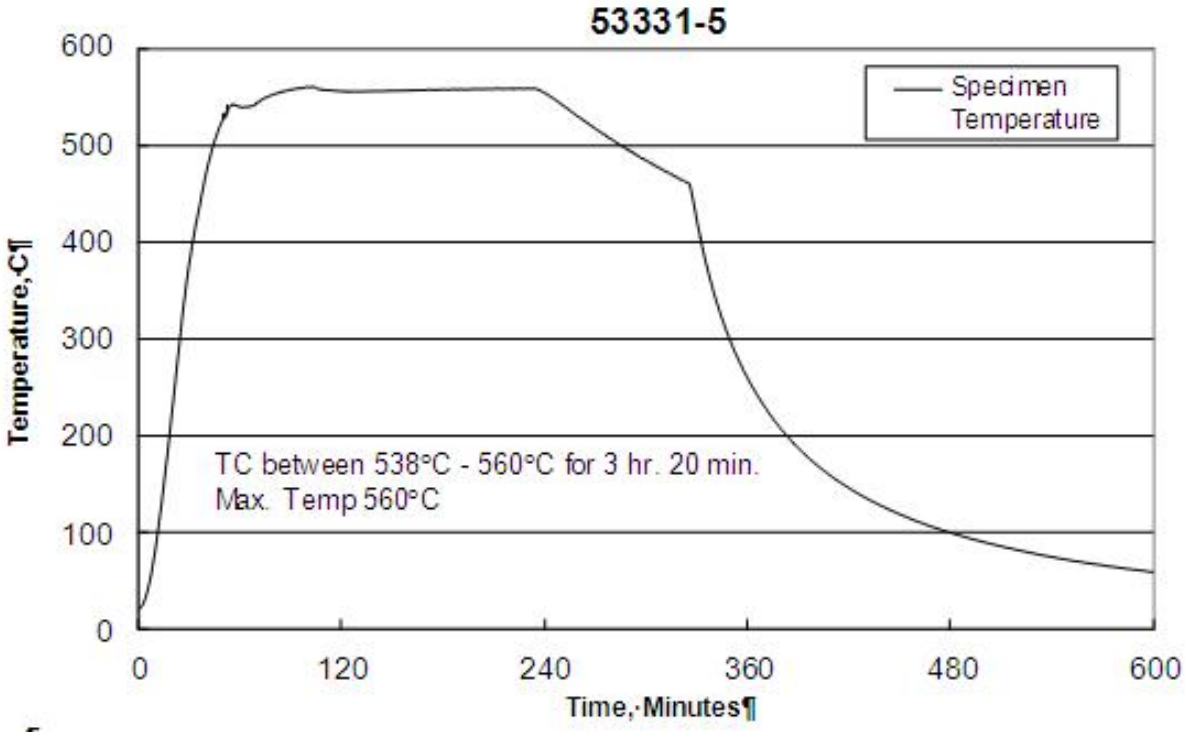

Figure 4. Bake Schedule for (ALL) Specimens

Figure 5 through Figure 8 show the specimens just prior to corrosion exposure.

Figure 5. PD Two-Step Treated Sample Set

Figure 6. ALL Three-Step Treated Sample Set

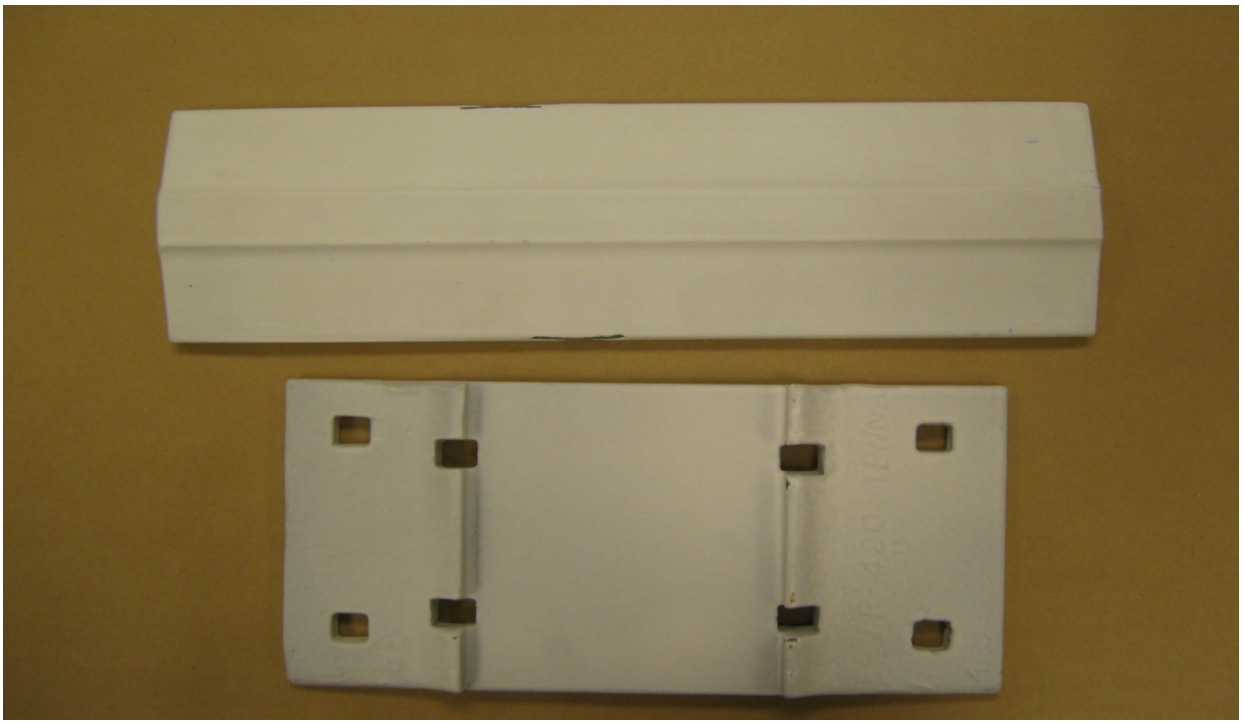

Figure 7. EonCoat® Treated Sample Set

Figure 8. No Treatment Flange Base

2.2.2 Corrosive Environment Exposures

The schedule for exposure is given in Table 3.

Table 3. Corrosion Exposure Schedule

Corrosion Cycles							
Week 1	Tues	Weds	Thurs*	Fri	Sat	Sun	Mon*
Day	**8-Jan**	9-Jan	**10-Jan**	**11-Jan**	12-Jan	13-Jan	**14-Jan**
Exposure	Salt water	Salt water	Dry (out)	Humidity	Humidity	Humidity	Dry (out)
Week 2	Tues	Weds	Thurs*	Fri	Sat	Sun	Mon*
Day	**15-Jan**	16-Jan	**17-Jan**	**18-Jan**	19-Jan	20-Jan	**21-Jan**
Exposure	Salt water	Salt water	Dry (out)	Humidity	Humidity	Humidity	Dry (out)
Week 3	Tues	Weds	Thurs*	Fri	Sat	Sun	Mon*
Day	**22-Jan**	23-Jan	**24-Jan**	**25-Jan**	26-Jan	27-Jan	**28-Jan**
Exposure	Salt water	Salt water	Dry (out)	Humidity	Humidity	Humidity	Dry (out)
	Bold days-samples get moved						
	*Thursdays and Mondays, take pictures of interfacial regions						

The saltwater solution was fixed at 5 percent by weight in a water solution of road deicing salt in tap water. Deicing salt contains magnesium chloride and calcium chloride in addition to the predominant sodium chloride. When the samples were first placed in saltwater, the PD system began to bleed blue-black color. (This also happened with the small-scale test bars in Task 1.) It was found later that this only happened when first immersed. In subsequent weeks of exposure, there was no additional bleeding (see Figure 9).

Figure 9. PD Samples on First Exposure to Saltwater

The hot-wet exposure took place in a large temperature and humidity controlled cabinet set at 50^{o}C with saturated humidity. For the humidity exposures, the stacked specimens were placed into the controlled temperature-humidity cabinet, as shown in Figure 10. Notice it is possible for condensate from the upper samples to drip down onto the lower samples.

Figure 10. Placement of Samples in Humidity Cabinet

2.2.3 Sample for Drip Zone Protection

An additional test was added during Task 2 to examine the ability of the treatments to inhibit corrosion due to drip condensation. EWI prepared an additional specimen with the ALL treatment. For the humidity exposure, a "drip tent" was fashioned inside the chamber to collect and direct condensate onto the top surface. The saltwater soak was replaced by an additional 2 days of humidity exposure. The ALL treatment was applied to one half of the top and bottom surfaces for this exposure. The exposure schedule for the drip zone test is given in Table 4.

Table 4. Drip Zone Corrosion Cycles

Corrosion Cycles - Drip							
Week 1	Tues	Weds	Thurs*	Fri	Sat	Sun	Mon*
Day	**4-Feb**	5-Feb	**6-Feb**	**7-Feb**	8-Feb	9-Feb	**10-Feb**
Exposure	Humidity	Humidity	Out	Humidity	Humidity	Humidity	Dry (out)
Week 2	Tues	Weds	Thurs*	Fri	Sat	Sun	Mon*
Day	**11-Feb**	12-Feb	**13-Feb**	**14-Feb**	15-Feb	16-Feb	**17-Feb**
Exposure	Humidity	Humidity	Out	Humidity	Humidity	Humidity	Dry (out)
Week 3	Tues	Weds	Thurs*	Fri	Sat	Sun	Mon*
Day	**18-Feb**	19-Feb	**20-Feb**	**21-Feb**	22-Feb	23-Feb	**24-Feb**
Exposure	Humidity	Humidity	Out	Humidity	Humidity	Humidity	Dry (out)
	Bold days-samples get moved						
	Only one sample. Place flange down on bottom shelf.						
	Make inverted-Vee foil tent to drip condensate onto the top.						
	*Thursdays and Mondays, take pictures of interfacial regions						

2.2.4 Salt Fog Testing

EWI performed salt fog testing (ASTM B117) on a separate set of treated specimens. Specimens were produced from 4×12-inch plates of 1018 steel, approximately $^{3}/_{16}$-inch thick to accommodate the ASTM B117 test chamber. These specimens were treated using the EWI ALL processing as a primer and a subsequent overcoating of PPG® PSX-700 epoxy-silicate paint. PSX-700 is approved by the U.S. Navy for use in ballast tank lining for ships and may stay in service for years. Salt fog testing was included to benchmark the EWI ALL system as a primer with a high-performance corrosion protection barrier coating, such as the PSX-700. The EonCoat® was included to rank its performance against the latter. The samples were sent to an outside vendor for exposure to 5,000 hours of salt fog exposure following ASTM B117.

2.3 Task 3 – Crack Fatigue Propagation and Mitigation (Medium-Scale)

The purpose of this task was to test the combined effects of damage (notch), surface protection, and corrosion on the fatigue performance of lower flange sections of rail. Fatigue loading was applied with rollers in a four-point bending arrangement. The center rollers were spaced at 8 inches and contacted the top surface adjacent to the radius of the rail. The outside rollers contacted the lower surface of the flange at 16-inch spacing (see Figure 11). Testing was performed at about 7 Hz.

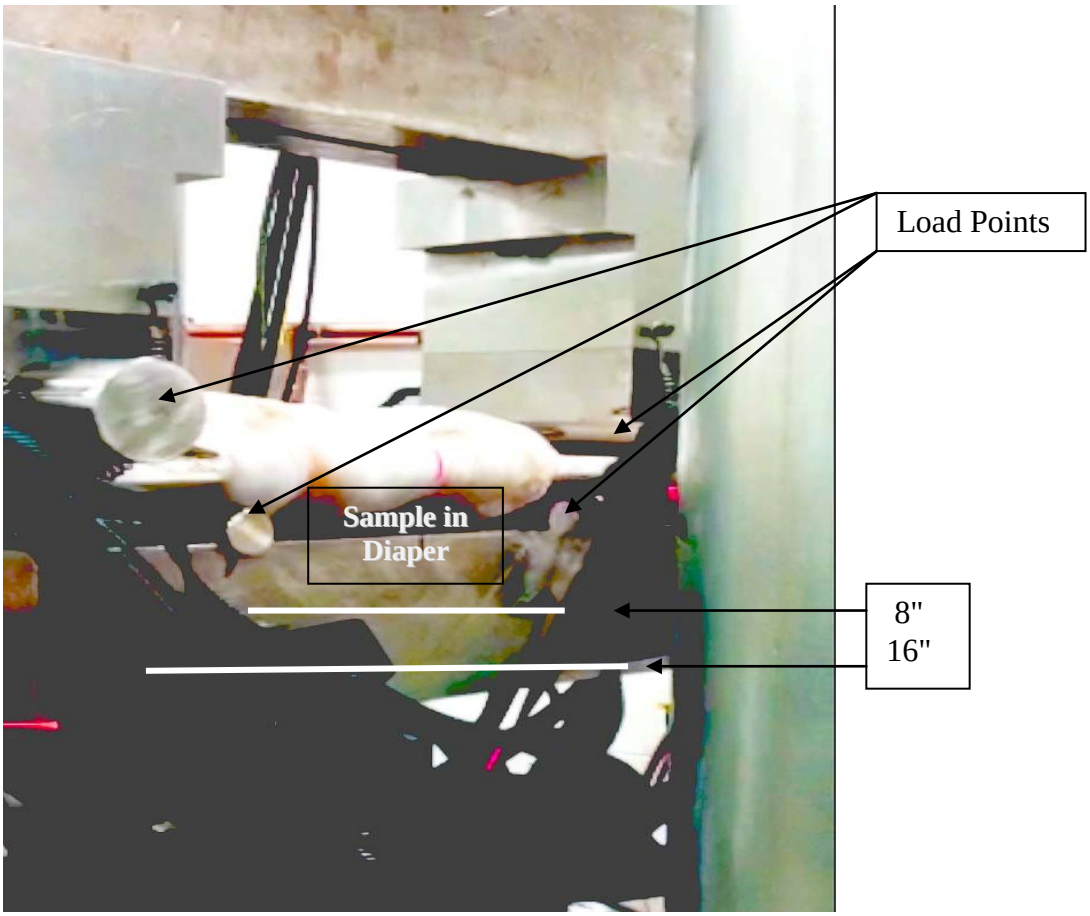

Figure 11. Four-Point Load Fatigue Test Setup

Table 5 lists the sample descriptions, applicable load ranges, and cycles to failure. The differing load ranges were required because of slight differences in sample geometries. When the heads and webs were removed from the rail stock, the position of the cut surface relative to the upturning radius of the flange-to-web junction differed from sample to sample. Some had cut faces leaving more residual web riser and others had been cut more deeply into the flange top surface. To provide the same nominal stress on the *lower* base flange surface during fatigue testing, different load levels were chosen for the top side loading to account for the differences in specimen size.

Corroded specimens were tested in the presence of topical, trapped saltwater (Samples #2-6). A saltwater "diaper" was emplaced to surround the notch region and was held in place with shrink wrap.

Table 5. Four-Point Load Fatigue Testing

Sample	Description	Corrosion Cycles	Load Range for R=0.1 (lbf)	Cycles to Failure	Comments
1	Un-notched, unprotected	N	15,755 - 1576	5,000,000	Run-out
2	Notched, unprotected	N	11,467 - 1147	305, 198	Failed at notch
3	Notched, unprotected, corrosion	Y	13,789 - 1379	61, 839	Failed at notch
4	Notched, 3-step, corrosion	Y	12,422 - 1242	218,514	Failed at notch
5	Notched, 2-step, corrosion	Y	12,422 - 1242	226,479	Failed at notch
6	Notched, EonCoat, corrosion	Y	13,322 - 1332	3,460,278	Stopped test (run-out)

2.4 Task 4 – Resonant Fatigue Testing (Rail Sections)

The purpose of this task was to look at the combined effects on full-scale rail segments and to determine if there was correlation between the medium-scale fatigue results and the fatigue results for longer rail sections. Twenty-foot rail sections of 136-pound rail were used for testing with a fatigue method called *resonant fatigue*.

2.4.1 Resonant Fatigue Methodology

Resonant fatigue methodology has been most commonly applied to testing welds in pipe and drill pipe used in oil exploration. It has been used on symmetrical, round cross sections. In the EWI adaptation, it was used on the asymmetrical cross section of a rail segment.

As applied here, a 20-foot section of rail was suspended between, and strapped to, two support points (Figure 12). Counterweights of calculated size were then attached to the ends. The cyclic excitation at close to the resonant frequency, provided by an eccentric drive cam at one end, forces the rail into self-resonance around the center line, creating what amounts to a standing wave on the rail with maximum stress in bending at the center of the length. The rail becomes an oscillator element.

Strain gauges monitor the cyclic strains at several locations on the part, but especially near the center. At some point, a crack will grow to sufficient size by fatigue to cause the rail to fracture. This is the failure point at which the machine stops and the cycles to failure are noted. In this case, the rail went into self-resonance at approximately 21 Hz. The applied stress level was determined by the difference between the resonant and excitation frequencies. The excitation and self-resonance induced a stress on the rail head of 28–40 ksi and a stress on the rail base of 25–26 ksi, for notched rail, not accounting for the additional stress concentration at the notch.

Figure 12. Rail Suspended in Resonant Fatigue Apparatus

Resonant fatigue of the rail provides reversed loading, represented as R=-1, where R is the ratio of minimum stress to maximum stress. Thus, the applied stress range is double the maximum stress of the cycle. The maximum stress is listed in tables and descriptions of this task. There were five test specimens for the resonant fatigue test.

1) RS1 − Plain rail segment, no notch or corrosion
2) RS2 − Notched, untreated, no corrosion
3) RS3 − Notched, untreated, corrosion
4) RS4 − Notched, treated with EWI three-step system, corrosion exposure
5) RS5 − Notched, treated with EonCoat®, corrosion exposure

2.4.2 Preparation of Rail Sections

Surface preparation methods and corrosion cycling for the 20-foot rail sections were modified from those used for partial rail segments to account for size. Surface rust was ground off to a distance of about 2 feet to either side of the center line on the bottom of the flange only. If notched, the notch was cut across the flange at the 10-foot point using a ceramic saw. (Unfortunately, this method does not allow for consistent notch dimensioning, which may have become a factor in skewing the results expected from the testing.)

Figure 13 shows a rail segment that has been treated with the EWI ALL three-step process and is wrapped with heater blankets prior to the bake cycle. An insulating layer of ceramic fiber blanket was then placed over the heating area. The rail section outside the insulated heating zone stayed quite cool.

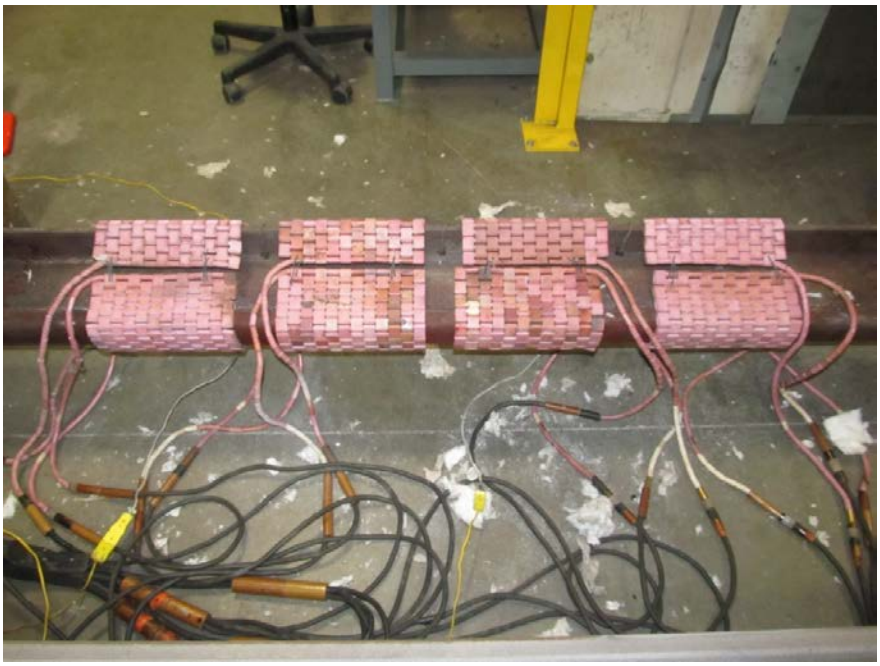

Figure 13. Resistance Heating Blankets used to Heat Cure Zirconia Sol-Gel Sealer

The vendor applied EonCoat® to the rail segment at EWI. Standard two-component spray equipment was used with a mixer-head nozzle (Figure 14). It dried within minutes of application. A second coat was then applied after approximately 10–15 minutes. That rail segment is shown in Figure 15. There was evidence of some debonding of the spray at the edges (circled in the figure). These locations were outside the prepared regions.

Figure 14. Technician Readies EonCoat® Applicator System

Figure 15. EonCoat® Sprayed Rail Segment

2.4.3 Corrosion Exposure Cycling for Large Rail Segments

The corrosion cycle followed that shown in Table 3 above. It was necessary to modify the corrosion cycling to adapt it to the large sample size. Soaking in a tank was impossible, for example, and the humidity exposure method required a change.

For the saltwater exposure, the rails were brushed with saltwater solution. Paper towels soaked in saltwater were then placed over the surface. A lofted fabric mat, also soaked in saltwater, was then overwrapped. That whole assembly was wrapped in place with shrink wrap to retain the solutions in contact with the rail and the notch region. This became the "diaper" to keep the saltwater solution in contact with the rail. For air drying, the diaper was cut off and discarded. To mimic the humidity chamber, the same basic diapering procedure was used, substituting water for salt water, to emulate the required 3-day humidity exposure. The cycle time lengths were the same as before and, overall, the exposure lasted 3 weeks.

No tie plates were used to trap liquid in the flange-to-plate gap during this corrosion cycle exposure.

3. Results and Discussion

3.1 Task 1 – Small-Scale Corrosion Exposure – Results and Discussion

3.1.1 Surface Studies

The purpose of Task 1 was to make a preliminary determination of which EWI two-step or three-step treatment systems might be effective in preventing or retarding surface corrosion on rail steel. The corrosive environment used in this program was highly aggressive and might not represent the effects of slower corrosion attack, as might be found in service. Therefore, the fact that aggressive corrosion exposure resulted in attack was not taken as an indication that the treatments were of no value.

At the end of each exposure week, photographs were taken of the bar samples to record their performance. All the samples exposed to corrosion showed rusting. This was not surprising given the severity of the exposure, especially the hot-wet portion, which is very aggressive when combined with a saline soak and interim drying.

Particular attention was paid to the condition of the bottom surface of the samples. This would be the area of most concern in a rail tunnel since it would not easily dry. Figure 16 and Figure 17 show the views of the bottoms of the samples after 2-week and 3-week exposure, respectively. Figure 18 and Figure 19 show the same samples, but for the top surfaces.

The samples were rated visually based on overall rust amount and severity, including blistering or flaking. The “PD” series and the “PDZ” series had replicates, so only one rating is given for each of those. The rating is from best to worst (1 to 4), as shown in Table 6.

One of the more striking observations was the degree of overall corrosion attack after 3 weeks compared with 2 weeks. The corrosion became quite aggressive during the third week. The results show that the ALL variant, which had the three-step application system with final bake, performed best in protecting the bottoms. However, the best performance for protecting the tops was the PD variant, which is a two-step process with no bake.

Figure 16. Bottoms of Samples after 2-Week Corrosion Cycle

Figure 17. Bottoms of Samples after 3-Week Corrosion Cycle

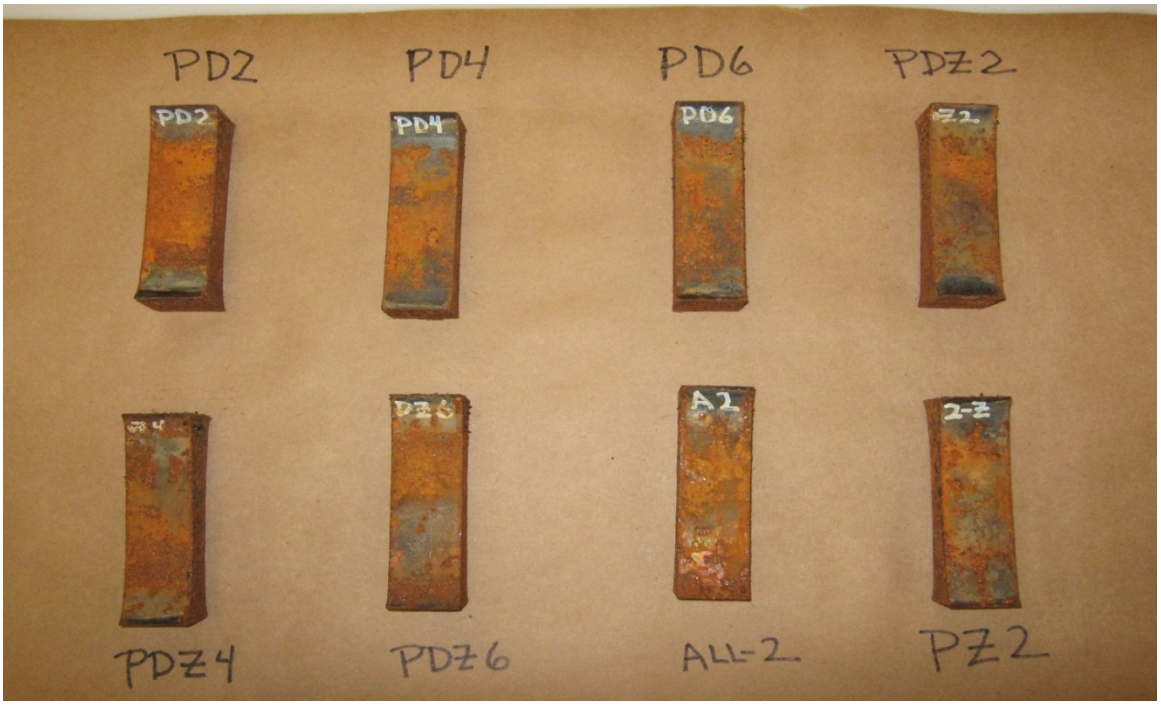

Figure 18. Tops of Samples after 2-Week Corrosion Cycles

Figure 19. Tops of Samples after 3-Week Corrosion Cycle

Table 6. Visual Interpretation of Corrosion Results

Sample Preparation						Tops						Bottoms		
						Ranking - after Salt Water			Ranking - after Hot/Wet			Ranking		
Corrosion	Phos	Dopa	Zirc	Bake	Total	Week 1	Week 2	Week 3	Week 1	Week 2	Week 3	Week 1	Week 2	Week 3
PD2	X	X			6	1	1	1	1	2	1	NR	3	2
PD4	X	X												
PD6	X	X												
PZ2	X		X	X	2	3	3	2	3	3	2	NR	2	3
Corrosion														
PDZ2	X	X	X		6	2	2	3	2	1	3	NR	4	4
PDZ4	X	X	X											
PDZ6	X	X	X											
ALL2	X	X	X	X	2	4	4	4	4	4	4	NR	1	1

Overall, the diphenol treatment (D) was more effective than diphenol (D) and zirconia (Z) combined (PD versus ALL2). The Z treatment in the absence of D was not as good when baked (PZ) compared with ALL. Therefore, some initial conversion treatment using D is important.

The specimens exposed to corrosion cycles (even numbered) were compared with their unexposed, treated counterparts (odd numbered) from the same sets. Three treated sets were chosen for the SEM/EDS analyses on unexposed and exposed samples.

1) PD series, which gave the best results on top surface corrosion resistance
2) ALL series, which gave the best results on bottom surface corrosion
3) PDZ series, which had the worst performance of all the combinations tried

3.1.2 Results from SEM/EDS Analyses

Samples were cut to provide test articles for scanning electron microscopy (SEM) and elemental x-ray dispersive (EDS) analyses. These were pieces taken from the center portions, as shown below (Figure 20 through Figure 23). The top sides were marked for orientation in the SEM instrument. The samples were analyzed using SEM to examine morphology. Integrated EDS capability was used to examine the coatings for chemical composition. The samples were examined both as cross cuts through the coatings ("sideways") and also on the tops themselves.

Figure 20. Photograph Summary of Samples for SEM/EDS Examination

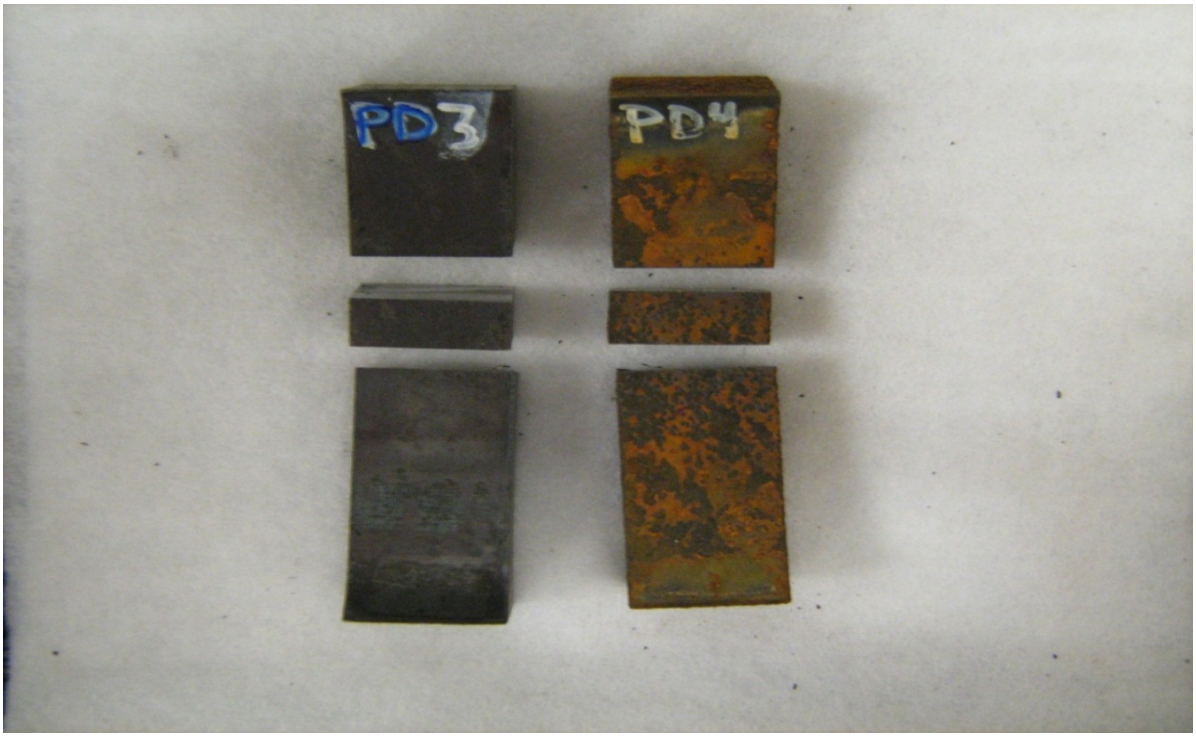

Figure 21. Close-Up of PD3/4 Series

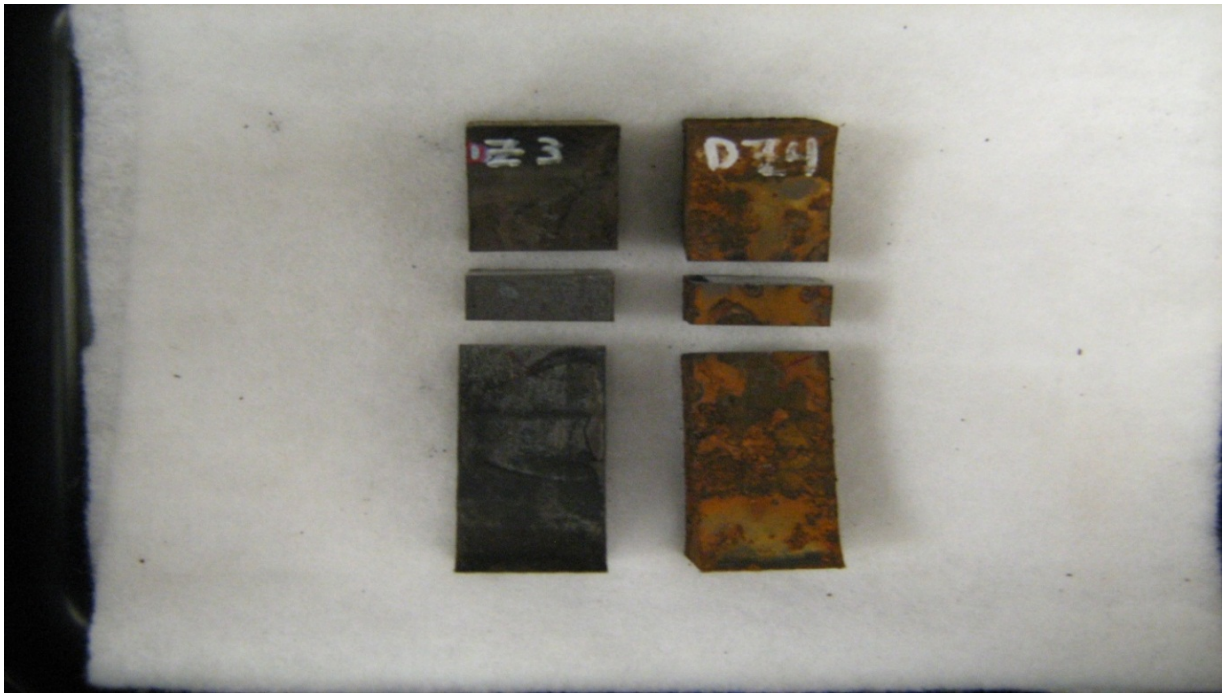

Figure 22. Close-Up of PDZ3/4 Series

Figure 23. Close-Up of ALL1/ALL2 Series

3.1.3 Crosscut Samples

For the following discussion, recall that odd-numbered sample types were treated, but not exposed to corrosion. Even-numbered sample types were treated and exposed to corrosion. Representative SEM photographs are shown for PD3 and PD4 (Figure 24), PDZ3 and PDZ4 (Figure 25), and ALL1 and ALL2 (Figure 26). These were taken at 1000× to accentuate the interfacial zones and the coatings themselves. The areas marked "Spectrum" show the scan locations for the EDS analysis.

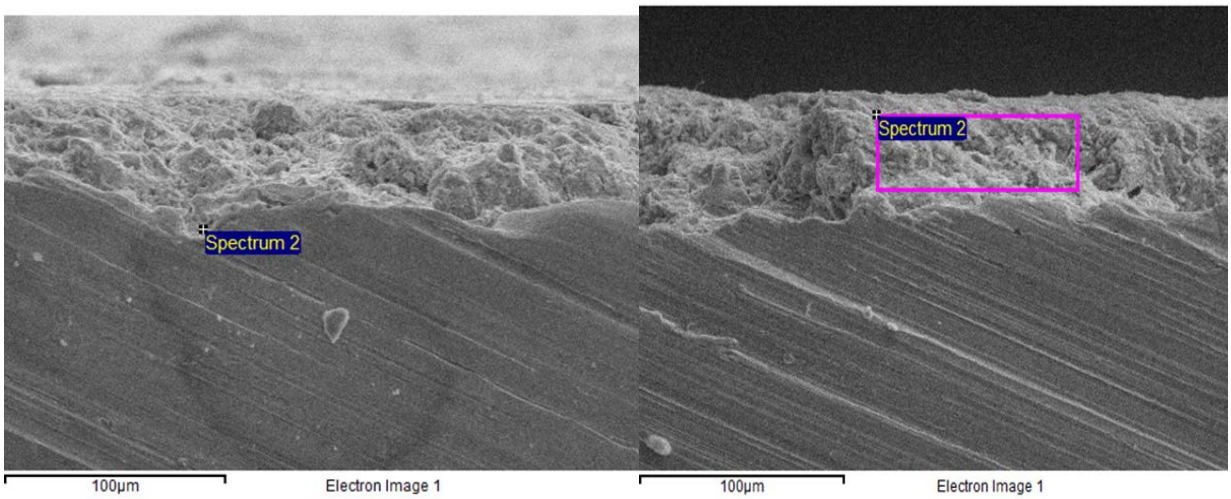

Figure 24. SEM Photographs of Cross Cuts for PD3 (Left) **and PD4** (Right)

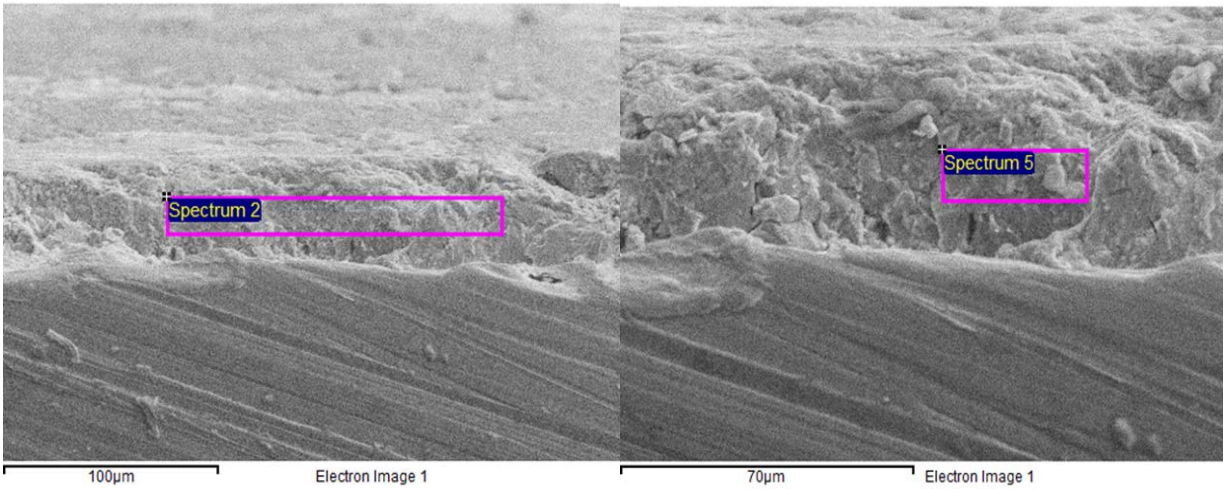

Figure 25. SEM Photographs of Cross Cuts for PDZ3 (Left) **and PDZ4** (Right)

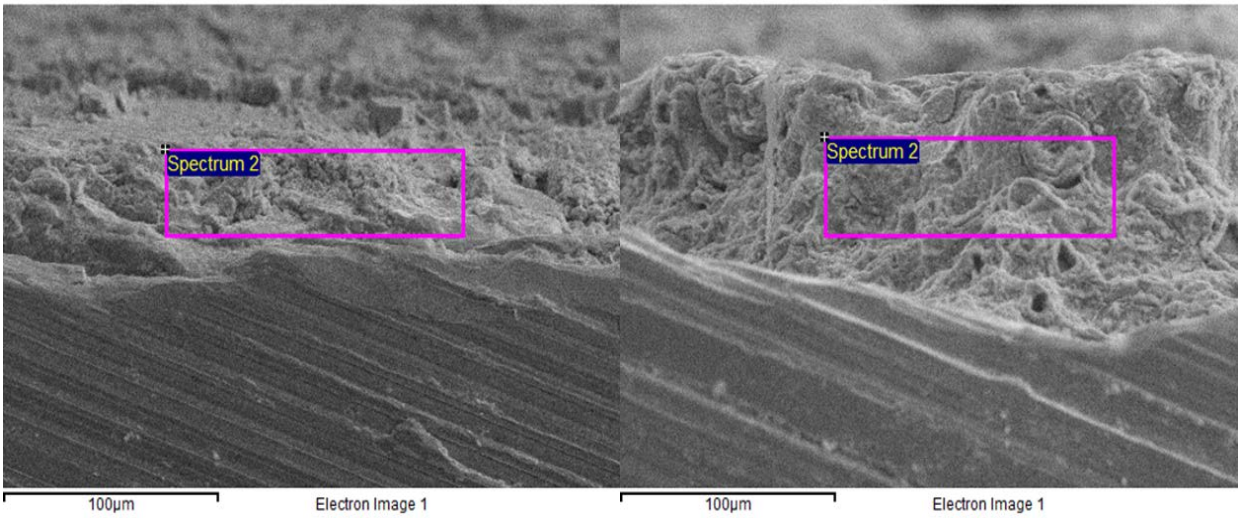

Figure 26. SEM Photographs of Cross Cuts for ALL1 (Left) **and ALL2** (Right)

All samples showed some porosity in the coatings. The EDS elemental analyses taken from cross cuts of the samples are provided in Table 7. There is significant iron content indicative of the ferrous/ferric material in the coatings and surface oxides. The predominance of iron (and also aluminum and silicon from the steel) is reflected in the low weight-percent of the other elements. The iron in these samples was 90–95 weight-percent of the total, meaning the other peaks were dwarfed.

The main interest was in finding evidence that the treatments used had changed the surface chemistry predictably, since the presence of phosphorous and zirconium would be expected. Other elements of potential interest were found in some cases, so they are reported below.

Table 7. Summary of EDS Analyses for Cross Cut Sample Coatings

Sample Preparation							EDS Analysis - Cross Section (Wt-%)			
2-step	Sample [Thickness (µ)]	Corrosion	Phos	Dopa	Zirc	Bake	P	Zr	Ca	Mn
	PD3 (44)	N	X	X						0.88
	PD4 (45)	Y	X	X						0.91
3-step	PDZ3 (41)	N	X	X	X			5.34		0.94
	PDZ4 (62)	Y	X	X	X		0.1	0.58	1.13	0.87
	ALL1 (48)	N	X	X	X	X	0.1	0.84		
	ALL2 (82)	Y	X	X	X	X	0.1	0.39		0.78

(P = Phosphorous; Zr = Zirconium; Ca = Calcium, Mn = Manganese)

The source of manganese is perplexing. It may have come from the bulk of the steel and been lifted into the coating during the phosphoric acid etch. Phosphorous and zirconium came from the treatments and were expected. The high level of zirconium in PDZ3 seemed anomalous given the

levels found elsewhere. The calcium was likely from the road deicing salt used in the saltwater exposure.

It is possible the calcium that appeared in PDZ4 was replacing the zirconium in the coating through ion exchange, resulting in depletion of the zirconium. The calcium was found mostly in nodules that appeared near and on the coating surface. Since PDZ3 and PDZ4 were not baked, the coatings could change in composition if chemical substitutions of other ions were possible. The ALL1 and ALL2 series were baked at 550°C, and the findings of P and Zr were not out of keeping with each other. No calcium appeared in the interior of that coating, suggesting possibly that ion exchange was discouraged by a more densified zirconium oxide coating formation.

Analyses of the cross cut samples indicate the treatments were effective in converting the surfaces, as hoped. However, ion exchange of calcium for zirconium appears to have taken place, rendering the protection of the zirconia seal coat ineffective. Calcium oxides are not particularly resistant to water attack or preventing chloride from reaching the iron surface.

3.1.4 Top Surface Analyses – Topology

The top surfaces were also examined using SEM. Representative SEM photographs of those samples are shown for PD3 and PD4 (Figure 27), PDZ3 and PDZ4 (Figure 28), and ALL1 and ALL2 (Figure 29). These were taken at 200× to give a larger view of the surfaces.

In general, the physical topologies were unremarkable. Cracking found in PDZ3 might be from the zirconia sol-gel. Sol-gels are susceptible to mud-cracking if dried or condensed too rapidly. Localized thickness variations leading to drying stress can also cause sol-gels to mud-crack as they dry and react. One might expect the same topology for PDZ4 as for PDZ3, since it was not baked, but that was not evident in the sample examined. As shown in Table 8, the amount of surface zirconium dropped in PDZ4 after the corrosive exposure. The mud-cracked zones could be expected to be more sensitive to "etching" so they may have been attacked preferentially during corrosion.

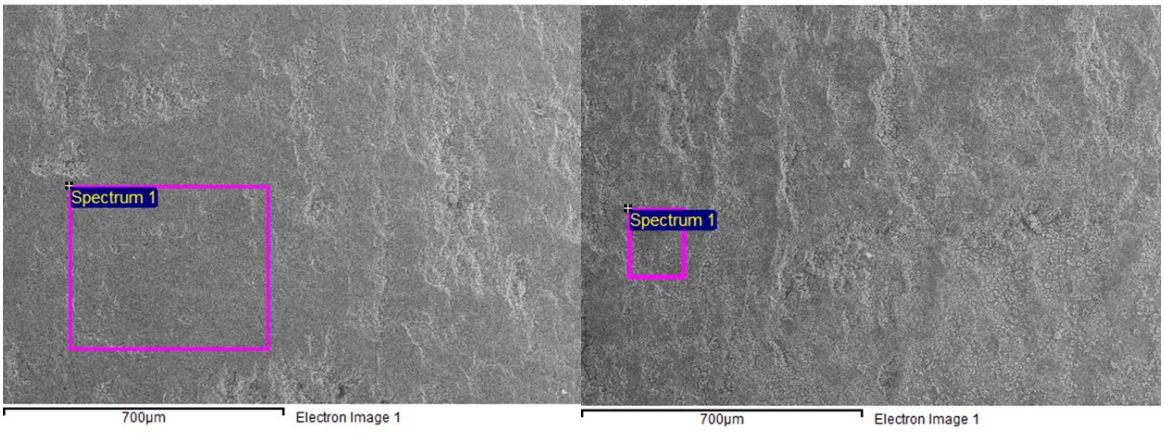

Figure 27. SEM Photographs of Top Surfaces for PD3 (Left) **and PD4** (Right)

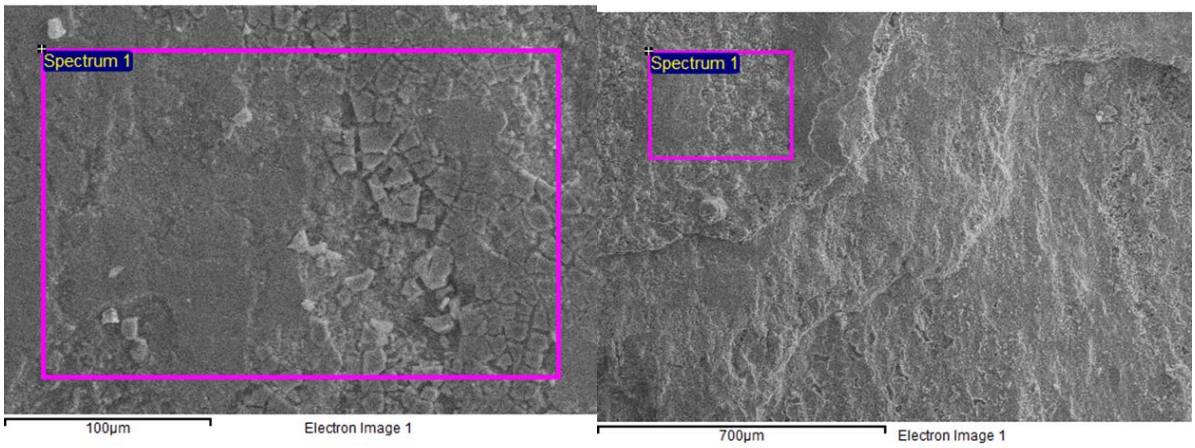

Figure 28. SEM Photographs of Top Surfaces for PDZ3 (Left) **and PDZ4** (Right)

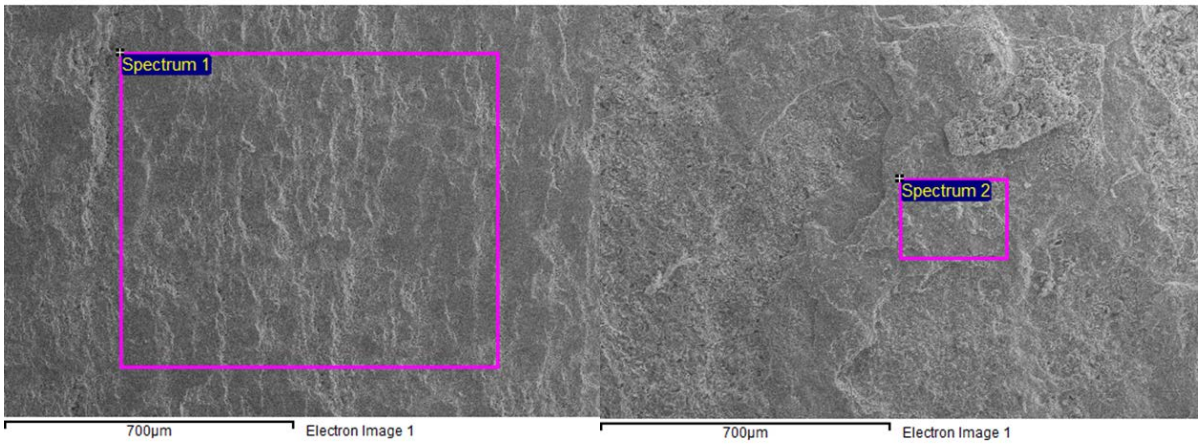

Figure 29. SEM Photographs of Top Surfaces for ALL1 (Left) **and ALL2** (Right)

3.1.5 Top Surface Analyses – Elemental Content

The surface chemistry of the coatings is important because that is the area affected by corrosive attack. The EDS elemental analyses for the top surfaces are summarized in Table 8.

Table 8. Summary of EDS Analyses for Sample Coating Surfaces

Sample Preparation							EDS Analysis - Top (Wt-%)			
	Sample	Corrosion	Phos	Dopa	Zirc	Bake	P	Zr	Ca	Mn
2-step	PD3	N	X	X			1.13		[0.55]	
	PD4	Y	X	X			1.52	[3.89]		
3-step	PDZ3	N	X	X	X		1.58	1.37		
	PDZ4	Y	X	X	X		0.42	0.42		
	ALL1	N	X	X	X	X	0.44	1.05		
	ALL2	Y	X	X	X	X			1.28	1.41

(P = Phosphorous; Zr = Zirconium; Ca = Calcium, Mn = Manganese)

There was a seemingly large peak for zirconium in PD4 which was unexpected since the PD-series was not treated with zirconia sol-gel. It is possible the zirconium leached from the PDZ3 and PDZ4 sample bars, which were unbaked. The unbaked sol-gel could have allowed leaching of Zr into the soak baths during the early soaking phases, possibly the first cycle of saltwater soak. The presence of calcium in PD3 was also unexpected since it was not exposed to deicing salt. The presence of calcium found in the top surface of ALL2 does not correlate with the analysis of ALL2 in the cross sections where none was found. Likely, it is topical from exposure to the saltwater and found only on the surface, again possibly due to ion exchange with zirconium, which was not found on the surface, but was found internally.

3.1.6 Implications for Protecting Rail Steel

In the previous EWI work,[6] the ALL system was used. It was very robust in ion-free water and survived 300°C water in an autoclave, exposed to approximately 1250 psi internal pressure. No rust formed. In this work, the availability of ionic species from the saltwater clearly had a different effect on the corrosion protection of the system. The significant finding of these analyses is that the topical treatments for the steel were effective in changing the surface chemistry, which was the desired intent. However, the combined protection of the ALL system and variants, while a partial hindrance to corrosion, did not protect against it. The overall effectiveness in protecting against corrosion varied, depending on the treatment.

Based on these findings, it was decided to proceed with the testing of some of the variants for coating larger samples. These were the PD two-step process and the ALL three-step process. The PD system was chosen because of its simplicity, requiring only two treatment materials and not requiring a bake. The ALL system was chosen because it represented the best EWI approach, which had borne out well in the previous studies involving water only.

3.2 Task 2 – Treatments on Rail Stock (Medium-Scale)

The sequential progress of corrosion is shown pictorially in Appendix A. A synopsis follows. At the end of the 3-week corrosion exposure, the PD, ALL, and untreated samples were corroded in varying degrees while the EonCoat® system showed virtually no corrosion (Figure 30 through Figure 33). The bottoms of the flanges and the tops of the tie plates are shown.

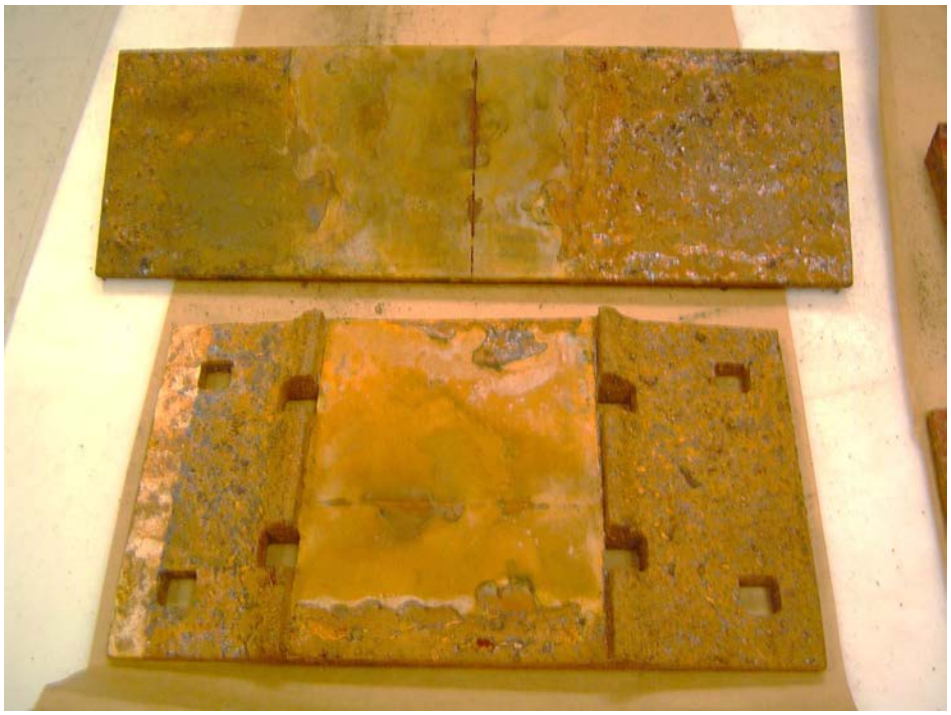

Figure 30. PD Treated Samples after 3-Week Exposure (Tie Plate and Flange Bottom)

Figure 31. ALL Samples after 3-Week Exposure

Figure 32. Untreated Samples after 3-Week Exposure

Figure 33. EonCoat® Samples after 3-Week Exposure

Based on visual examination, the EonCoat®-treated sample showed considerable resistance to the combined corrosion cycles. The rust spots on the EonCoat® surface were caused by condensate from the specimen on the shelf above it in the humidity cabinet. A beneficial observation was that areas of the EonCoat® that had been chipped or physically damaged in handling still did *not* succumb to corrosion attack.

In general, the time spent in humidity was very aggressive and most likely to produce the most sequential damage. Of interest concerning the samples treated with the ALL conversion system was the considerable protection between the flange bottom and the tie plate nested surface even in the presence of aggressive corrosion attack (Figure 31). The outer exposed portions of the samples were severely corroded.

The notches cut into flange bases before treatment and corrosion exposure showed varying degrees of rusting within the defect. The untreated samples were the most attacked, being almost rusted shut, while the sample with EonCoat® system was unaffected. The samples treated with the PD system and ALL system showed about the same level of corrosion within the defect zones, based on visual examination at 4×. There was little bridging rust in the latter samples where the rusting had progressed to where it was closing the gap for the untreated flange.

3.2.1 Drip Zone Samples

The results after 3 weeks for the top and bottom of the drip zone sample are shown in Figure 34 and Figure 35, respectively. In both cases, the protected portions were on the bottom half of the photographs. The protection on the bottom half of the top surface was fairly good. The protection for the trapped portion on the flange bottom was fair, but noticeable. There was possibly some benefit from the ALL treatment, and it might prolong rail life in actual service, but the protection was not dramatic.

Figure 34. Drip Zone Top Surface after 3 Weeks

Figure 35. Drip Zone Bottom Surface after 3 Weeks

3.2.2 Salt Fog Testing

Additional plate specimens had been prepared prior to this work using the EWI ALL processing as a primer on 1018 steel and a subsequent overcoating of PPG® PSX-700 epoxy-silicate paint. Samples coated with EonCoat® were also included to rank its performance against the latter. A total of six sample plates were exposed to ASTM B117 salt fog testing. The salt fog testing and specimen photographs are detailed in Appendix B.

The results indicate that the EWI three-step (ALL) process may be useful as a primer underneath a barrier-type coating; but, the EonCoat® system itself provided better overall corrosion protection.

3.3 Task 3 – Crack Fatigue Propagation and Mitigation (Medium-Scale)

The samples prepared and exposed in Task 2 were subjected to four-point load fatigue testing. The results for the four-point load fatigue testing are given in Table 9.

With the first three samples, a flange segment having no damage or corrosion (#1) did not fail after 5,000,000 cycles. Testing was stopped and this was considered run-out. Sample #2 was notched on the base (damaged), but had no corrosion cycles and failed at ~300,000 cycles. Thus, the damage itself reduced fatigue life by approximately one order of magnitude. The added effect of corrosion (#3) dropped the result almost another order of magnitude to ~60,000 cycles. This suggests the combined effects of damage, corrosion, and fatigue have a severe impact on rail fatigue life.

Table 9. Fatigue on Medium-Scale Samples

Sample	Description	Corrosion Cycles	Load Range for R=0.1 (lbf)	Cycles to Failure	Comments
1	Un-notched, unprotected	N	15,755 - 1576	5,000,000	Run-out
2	Notched, unprotected	N	11,467 - 1147	305, 198	Failed at notch
3	Notched, unprotected, corrosion	Y	13,789 - 1379	61, 839	Failed at notch
4	Notched, 3-step, corrosion	Y	12,422 - 1242	218,514	Failed at notch
5	Notched, 2-step, corrosion	Y	12,422 - 1242	226,479	Failed at notch
6	Notched, EonCoat, corrosion	Y	13,322 - 1332	3,460,278	Stopped test (run-out)

For the corrosion-protected samples, the ALL (three-step) and DP (two-step) treatment processes both showed the ability to offer some benefit in fatigue life from protection in severe corrosive environments. Samples #4 and #5 showed a reduction in fatigue life of approximately 30 percent compared with Sample #2, but a significant improvement in fatigue life over Sample #3 (no protection). Of the three protected samples, the EonCoat® system (#6), effectively gave run-out under fatigue, meaning it showed very good ability to prevent corrosive damage and allow a longer fatigue life.

In comparing Sample #6 with Sample #2, the question may arise as to why Sample #6 lasted so much longer than Sample #2, which had no corrosion protection. As mentioned, the test samples were fatigued in the presence of saltwater. Visual examination showed the presence of rust formation in the crack zone of Sample #2. It is postulated that the unprotected Sample #2 actually experienced an unintended corrosive attack during the test, resulting in reduced fatigue life.

All the corrosion protection methods showed some benefit in extending fatigue performance on notched samples exposed to corrosion. The largest improvement came from the EonCoat®, while the other two treatment methods improved fatigue life, but not as dramatically. Both those treatments showed similar performance and life extension.

The fracture surfaces for Sample #2 (NONE) and Sample #4 (ALL) are shown in Figure 36 and Figure 37, respectively. Notice the advance of corrosion in the damage zone is greater for the sample with no protection than for the sample with corrosion protection.

Figure 36. Fracture Surface of Corroded Sample with No Protection

Figure 37. Fracture Surface of Corroded Sample with ALL Treatment

The results of the four-point load fatigue tests were in keeping with expectations. For this work, only one sample of each type was tested. A traditional S/N curve was not developed. The goal was to look for trends. Future work with more focus on sample size and statistical performance could be appropriate for a subsequent phase. From this work, it appears the influence of damage on fatigue life is to reduce it about one order of magnitude. Added corrosion can reduce fatigue life by roughly an additional order of magnitude. In other words, pernicious corrosion combined with damage and fatigue can significantly reduce rail life.

3.4 Task 4 − Resonant Fatigue Testing (Rail Sections)

The resonant fatigue test can be compared with three-point bend and four-point bend fatigue tests, as well as with rolling load tests, since all these tests can be performed on scales similar to those used in this work. Fatigue tests can be performed on samples ranging from small coupons to a test of rail in place, as at the Facility for Accelerated Service Testing (FAST) loop. Because of its high cycle rate, resonant fatigue testing has the potential to perform the testing more quickly than similar scale tests and places peak bending stresses at both the top and bottom surfaces of the rail instead of only at one or the other. Resonant fatigue uses a longer sample of rail than similar scale tests, but also stresses a longer area with a nearly uniform stress distribution. Like three- and four-point bend tests, resonant fatigue does not allow for the contact of the rail wheel with the rail head. It is potentially useful for checking behavior where contact forces are not an issue. If contact forces are an issue, then a rolling load test is more appropriate.

The results of the resonant fatigue testing are summarized in Table 10 and Figure 38.

Table 10. Summary of Resonant Fatigue Testing

Sample	Description	Corrosion Cycles	Rail Head Stress (ksi)	Rail Base Stress (ksi)	Cycles to Failure	Comments
RS1	Un-notched, unprotected	N	39.6	32.9	840,613	No failure
RS2	Notched, unprotected	N	28.6	25	109,888	Fracture from fatigue crack at notch
RS3	Notched, unprotected, corrosion	Y	30	26.4	133,291	Fracture from fatigue crack at notch
RS4	Notched, 3-step, corrosion	Y	29.3	26.3	967,968	No failure, but rusted
RS5	Notched, EonCoat, corrosion	Y	29.8	25.7	94,745	Fracture from fatigue crack at notch

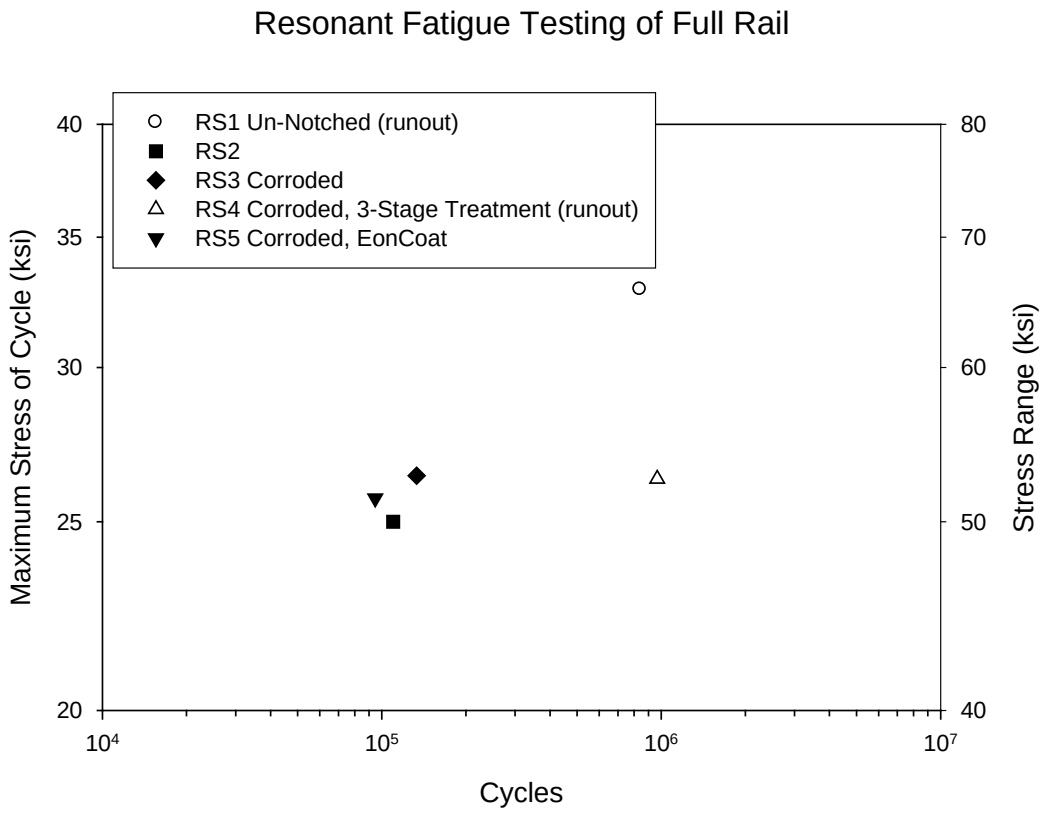

Figure 38. Resonant Fatigue Test Lifetime Results

One of the more significant findings of this test was that asymmetrical cross sections, such as rail, could be induced to self-resonate by this method. Previously, only circular cross sections (i.e., pipe and girth welds) had been tested with resonant fatigue, and the ability to put rail segments into oscillation was noteworthy.

Fatigue results are judged partly based on the range of stress loading. Since the cycles provide reversed loading, the stress ranges will be twice the values given in Table 10, or roughly 60–80 ksi. Sample RS1 was tested without a notch and at a higher stress range than the notched rails. Failure of that sample was not induced in the testing. Samples RS2–RS5 were pre-notched before treatments, corrosion cycles, or testing. RS2 was not protected from corrosion, but it also did not see purposeful corrosion cycles. Sample RS3 was unprotected, but *did* undergo corrosion cycling and had a saltwater solution "diaper" applied during resonant fatigue. It could represent older rail in service that had somehow been damaged and suffered corrosion attack. It failed in the crack zone, but showed slightly higher fatigue life despite the corrosion and lack of protection. Rust formation is clearly evident in the failure zone of RS3 (Figure 39).

Figure 39. Resonant Fatigue Fracture Surface of Unprotected, Corroded Rail (Sample RS3) Arrow Shows Crack Zone

The EonCoat®-treated sample (RS5) showed approximately the same number of cycles to failure as the notched untreated sample that had not been corroded (RS2) and the notched untreated sample that had been corroded (RS3). This comparison suggests corrosion has *no* effect on rail fatigue life, which is in conflict with the four-point load results found in Task 3. The differences in fatigue life found for the notched samples RS2, RS3, and RS5 are not statistically significant. This suggests that damage, corrosion, and corrosion protection are *not* interconnected in fatigue-related phenomena, a conclusion which sharply contrasts with the fatigue results found for the four-point load testing used on the medium-scale samples. These samples also do not correlate intuitively with anticipated fatigue life behavior.

Because sample RS4 did not fail within expected test duration, that test run was suspended. This was also surprising and unexpected. Sample RS4 was notched and had the EWI three-step corrosion protection applied prior to being subjected to corrosion cycles. It also had the saltwater diaper applied during resonant fatigue. It did not fail during testing, reaching nearly one million cycles without failure, which conflicted with expectations and did not mirror the results found with the four-point load testing. The notch in RS4 showed minimal corrosion, with the least amount of corrosion in the center of the flange width and more at the tips of the flange.

In comparing the character of the fracture surfaces with those for the medium-scale samples, the resonant fatigue samples showed much smaller regions of fatigue cracking than those visible on the medium-scale samples (Figure 40 and Figure 41, tested in Task 3). This difference is attributed to the larger cross-section of the full rail inducing a higher stress intensity factor in the rail at the fatigue crack tip, allowing brittle fracture to take over from fatigue at a smaller crack size.

Figure 40. Fracture Surface of Corroded Sample with No Protection (Crack – corrosion area is circled)

Figure 41. Fracture Surface of Corroded Sample with ALL Treatment

It is disappointing that resonant fatigue testing did not provide predictable correlation. It was hoped this technique might be useful as a general, and fairly inexpensive, screening tool for examining rail fatigue behavior prior to submitting to more time-consuming field trials. It was not meant to replace those trials, but to enable reducing the number of samples needed in trial by first culling those destined to give poor results. This was not the case; therefore, the testing was of no predictive value.

If the reliability of the technique is governed by notch dimension and quality, a more thorough study would be needed to determine the notch dimensions and even where it should be placed. The technique may ultimately be of value. Further testing using statistically significant numbers of samples would be useful in making a final determination about the potential for this technique.

4. Conclusions and Recommendations

4.1 Conclusions

An organometallic conversion type coating system, investigated at EWI for use in high pressure liquid water systems, was useful in retarding the effects of corrosion on fatigue rail life. However, it did not prevent corrosion in the presence of saltwater or condensing humidity. A commercially available inorganic conversion coating (EonCoat®) was effective in preventing corrosion in saltwater environments. It enabled extended fatigue life, even on damaged rail subjected to aggressive corrosive environments, and gave performance similar to that for undamaged, uncorroded rail.

In this work, it was found that the interactions between rail damage, corrosive attack, and overall rail fatigue life can be examined by methodical application of traditional four-point fatigue testing using manageable sample sizes. The influences of corrosion and damage in the presence of fatigue stress are believed to be separable based on this limited testing. The presence of damage alone reduces rail fatigue life by as much as one order of magnitude. Added corrosion attack reduced fatigue life by as much as an additional order of magnitude. The combined effects on rail life of damage, corrosion, and fatigue can be severe. Use of corrosion protection systems, applied to the base of the rail flange, can extend rail fatigue life.

A resonant fatigue test method was adapted for use with 20-foot long rail segments. It was shown that asymmetrical and heavy cross sections could, in fact, be induced into self-oscillation, developing approximately 60–80 ksi peak stress. In this work, the method was not found to be predictive regarding fatigue life for damaged, corroded rail, with or without corrosion protection. However, rail was taken to failure by this method, suggesting a more advanced test methodology might be useful for screening rail fatigue phenomena.

4.2 Recommendations for Future Work

This program was initiated in response to the specific issue of track damage and derailment resulting from corrosive underside attack to the rail. The intent of the program has always been to proceed to on-track evaluation of the potential anti-corrosion system. Therefore, a monitored field trial of the EonCoat® system is highly recommended. A substantive test should involve five to seven select trial installations representing different levels of potential corrosion attack, based on track location and traffic load.

Further, the four-point fatigue data gathered, while indicative of the potential for success, is minimal. Now that a preliminary recommendation has been achieved, continued four-point load fatigue testing involving a more statistically significant sample population should be undertaken, focusing on the EonCoat® system as the protective material. This testing would include continued use of corrosion exposure. Further attention must be paid to the dimensions and machining accuracy of the notches. Essentially, this would replicate Task 2 and Task 3 with a larger population of samples, arriving at an actual stress range versus number of cycles (S/N) plot for each condition.

Finally, it is still believed that the resonant fatigue testing method has the potential to be a cost-effective test tool. First, the methodology should be improved to be consistently predictive of fatigue behavior within a given sample set featuring different kinds of abuse. Particular attention should be paid to notch dimensions and placement. Once the methodology is internally self-consistent, a method should be found to correlate those results with those found in the field; for example, placing rail having similar abusive history on fast track, which would enable the resonant fatigue method to become truly predictive.

5. References

(1) Robles-Hernandez, F.C.; Koch, Kevin; Plascencia-Barrera, Gabriel. Rail Base Corrosion Detection and Prevention. *TCRP Web Only Document 37*, March 2007.

(2) Robles-Hernandez, F.C., Plascensia, G., Koch, K. "Rail Base Corrosion Problem for North American Transit Systems," Engineering Failure Analysis 16(1), 2009, p. 281–294.

(3) Robles-Hernandez, F.C., Kock, K. "Rail-base Corrosion Analysis: A Major Factor that Shortens Service Life of Rail in North American Transit," TMS Annual Meeting, p. 39–54, 2007.

(4) Akhtar, Muhammad. Guidelines for Rail Base Inspection and Rail Condemnation Limits for Corrosion Induced Material Loss. *TCRP Web Only Document 47*, March 2009.

(5) Panda, Bijayani; Balasubramanium, R.; Dwivedi, Gopal. On the Corrosion Behavior of Novel High Carbon Rail Steels in Simulated Cyclic Wet-Dry Salt Fog Conditions. *Corrosion Science*, 50(6), 1684–1692, June 2008.

(6) EWI Research report for Project No. 52684GTH.

(7) EonCoat LLC, 4000 Airport Drive, Wilson, NC, 27896.

(8) H. Li, K. Liang, L. Mei and S. Gu, "Oxidation Resistance of Mild Steel by Zirconia Sol-Gel Coatings," Mater. Sci. and Eng. A, 341, 2003, p. 87–90.

Appendix A. Pictures of Corrosion Samples from Task 2

Fig. A-1. Week 1 – PD after Salt Water

Fig. A-2. Week 1 – PD after Humidity

Fig. A-3. Week 2 – PD after Salt Water

Fig. A-4. Week 2 – PD after Humidity

Fig. A-5. Week 3 – PD after Salt Water

Fig. A-6. Week 3 – PD after Humidity

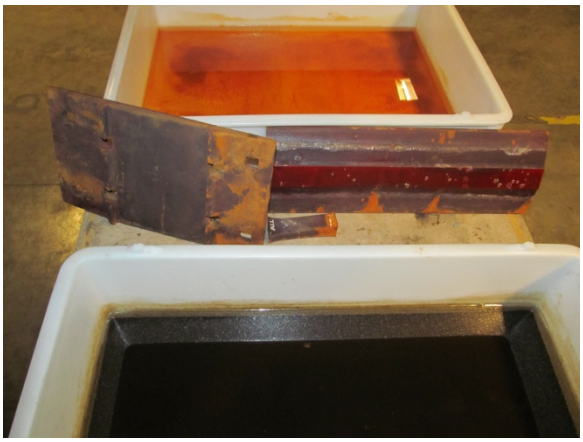

Fig. A-7. Week 1 – ALL after Salt Water

Fig. A-8. Week 1 – ALL after Humidity

Fig. A-9. Week 2 – ALL after Salt Water

Fig. A-10. Week 2 – ALL after Humidity

Fig. A-11.Week 3 – ALL after Salt Water

Fig. A-12.Week 3 – ALL after Humidity

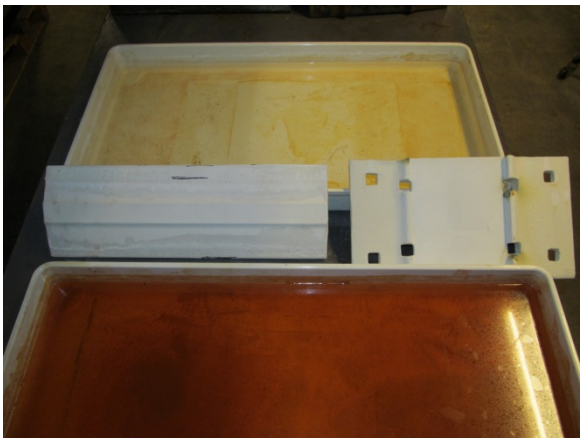

Fig. A-13. Week 1 – EC after Salt Water

Fig. A-14. Week 1 – EC after Humidity

Fig. A-15. Week 2 – EC after Salt Water

Fig.A-16. Week 2 – EC after Humidity

Fig. A-17. Week 3 – EC after Salt Water

Fig. A-18. Week 3 – EC after Humidity

Fig. A-19 Week 1 – No Treat, Salt Water

Fig. A-20. Week 1 – No Treat, Humidity

Fig. A-21 Week 2 – No Treat, Salt Water

Fig. A-22. Week 2 – No Treat, Humidity

Fig. A-23. Week 3 – No Treat, Salt Water

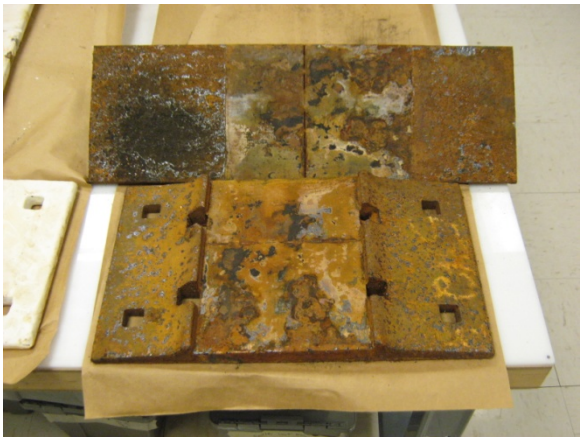

Fig. A-24. Week 3 – No Treat, Humidity

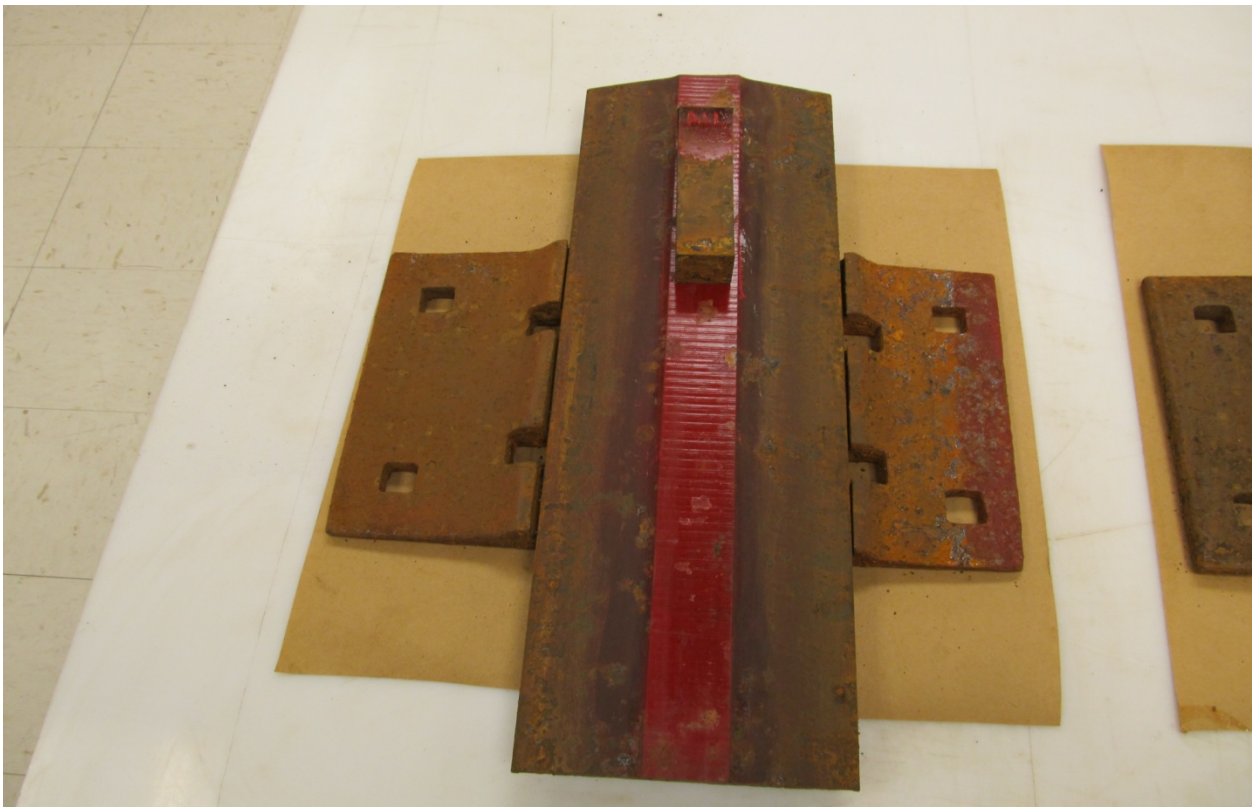

Figure A-25. ALL after Cleaning

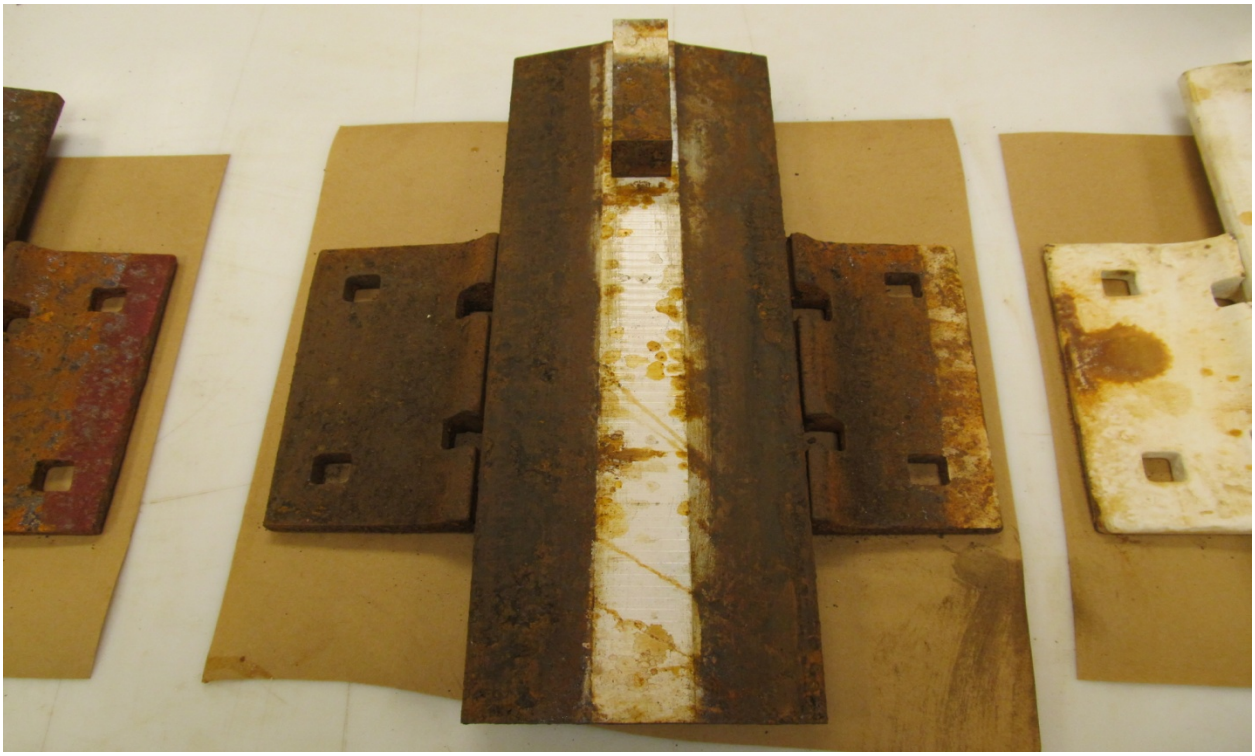

Figure A-26. PD after Cleaning

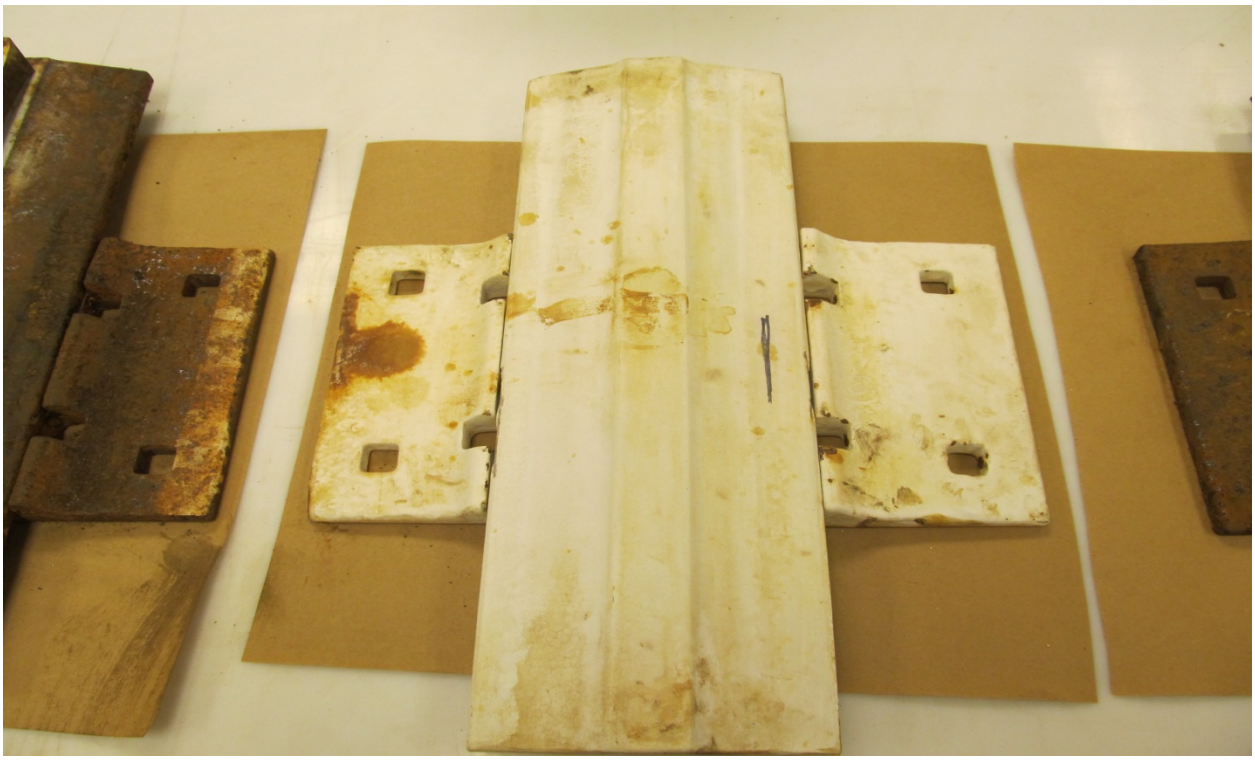

Figure A-27. EonCoat® after Cleaning

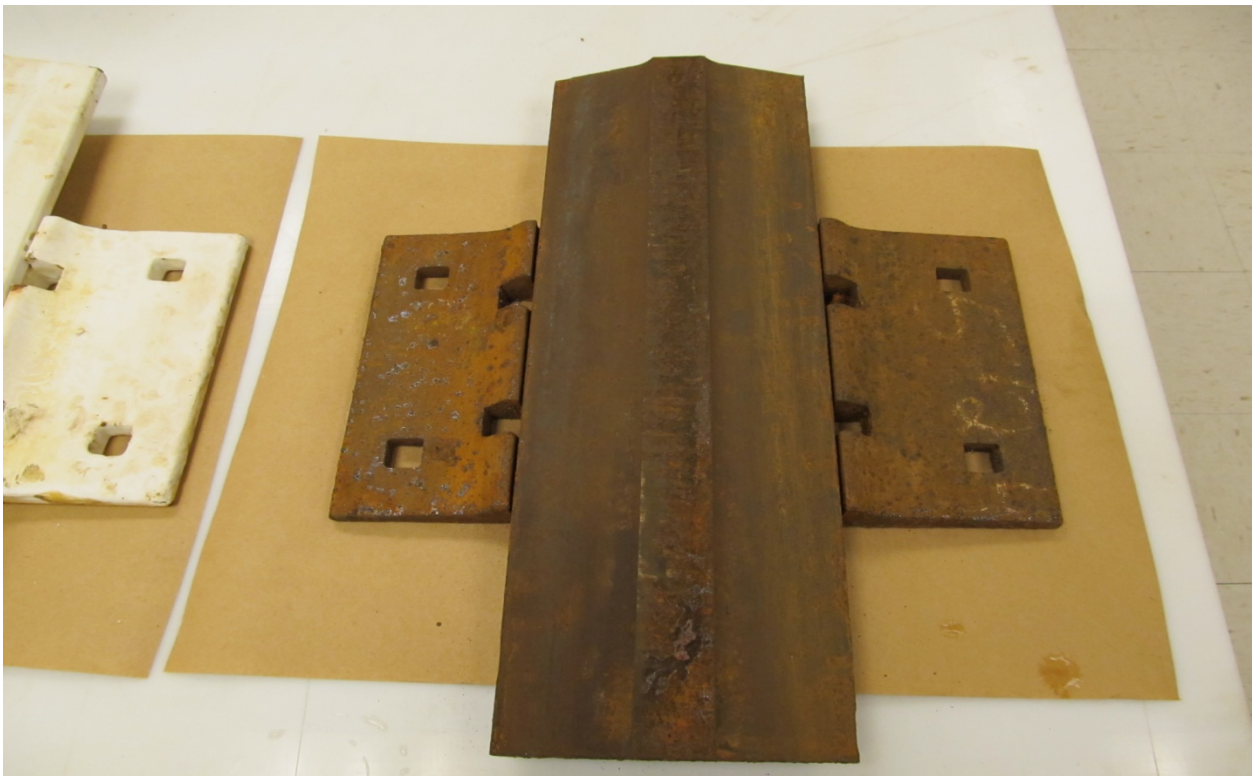

Figure A-28. No Treatment, after Cleaning

Appendix B. Salt Fog Testing

Salt fog testing (ASTM B117) is a highly aggressive procedure for examining the relative corrosion resistance of treatments on metals. Previously, EWI had prepared four 4x12-inch sample plates of 1018 steel, treated with the EWI ALL three-step process and coated with PPG® PSX-700 epoxy-silicate paint. This is a high-build material which meets U.S. Navy specification for use inside ballast tanks. Two additional plates were treated with EonCoat® only by the vendor.

This testing can performed in two ways. All the plates are first completely coated, including the edges. The first test consists simply of placing them in the test chamber for the requested number of exposure hours. The second method is to purposely scribe through the coating to get to bare metal. In the first case, the absolute barrier protection of the coating can be visually examined. In the second case, the amount of developed rust and its undercutting of the metal underneath the coating are examined. The second method enables a ranking based on how well the coating protects the surrounding area from creeping damage once initial damage has taken place. For this testing, both methods were used. One face was left coated and the other was scribed. The same plates therefore allowed for a total of twelve exposure types: eight for the EWI system and four for the EonCoat®.

The purpose for including this testing was to examine the absolute corrosion protection ability of the two systems, regardless of whether or not they were applied to rail. The specified time increments were 500 hours, 1,500 hours, 3,000 hours, and 5,000 hours for the EWI system with PPG® PSX-700. The EonCoat® samples were exposed for 500 and 5,000 hours. A pictorial summary follows.

After 500 hours, the EWI sample showed attack on the scribed side (Figure B-1), while the EonCoat® system showed very little attack. After 5,000-hour exposure (Figure B-2) the EWI system sustained significant damage with undercutting and blistering, whereas the EonCoat® system was still holding up very well and offering good protection.

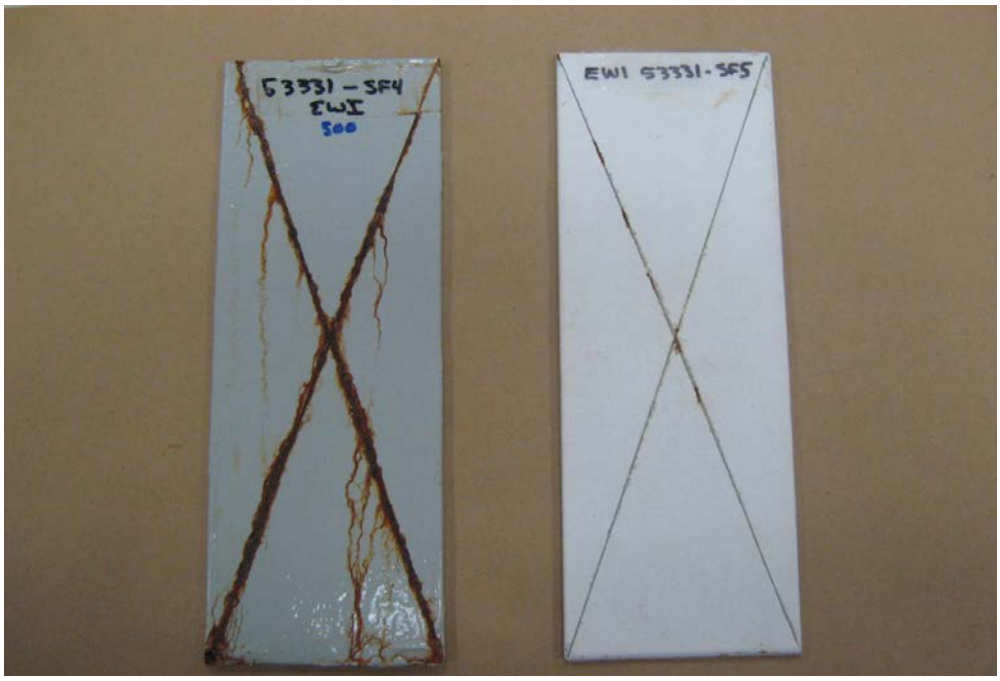

Figure B-1. EWI (left) and EonCoat® (right) after 500 Hours, Scribed to Metal.

Figure B-2. EWI (left) and EonCoat® (right) after 5000 Hours, Scribed to Metal

After 5,000 hours, the back sides (Figures B-3) were showing delamination for the EWI system, but there was still residual protection on the exposed metal. This suggests the EWI system as a primer can continue to provide protection even if the top coat is dislodged, as long as the primer is intact (not scribed or damaged).

The progression of front, scribed side attack on the EWI system is shown in Figure B-4. Once the primer is destroyed, it does not function effectively. The back side for EonCoat® shown at 500 hours and 5,000 hours in Figure B-5 shows the possible onset of progressive loss in effectiveness. However, the overall protection appears to be quite good.

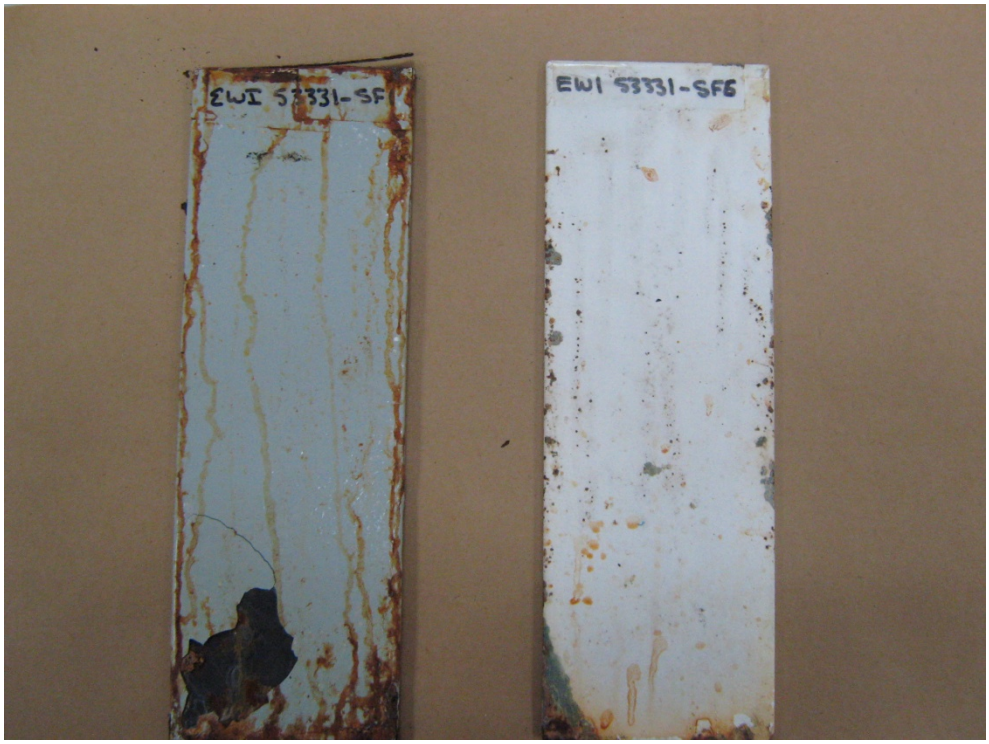

Figure B-3. EWI (left) and EonCoat® (right) after 5,000 Hours, Back Side

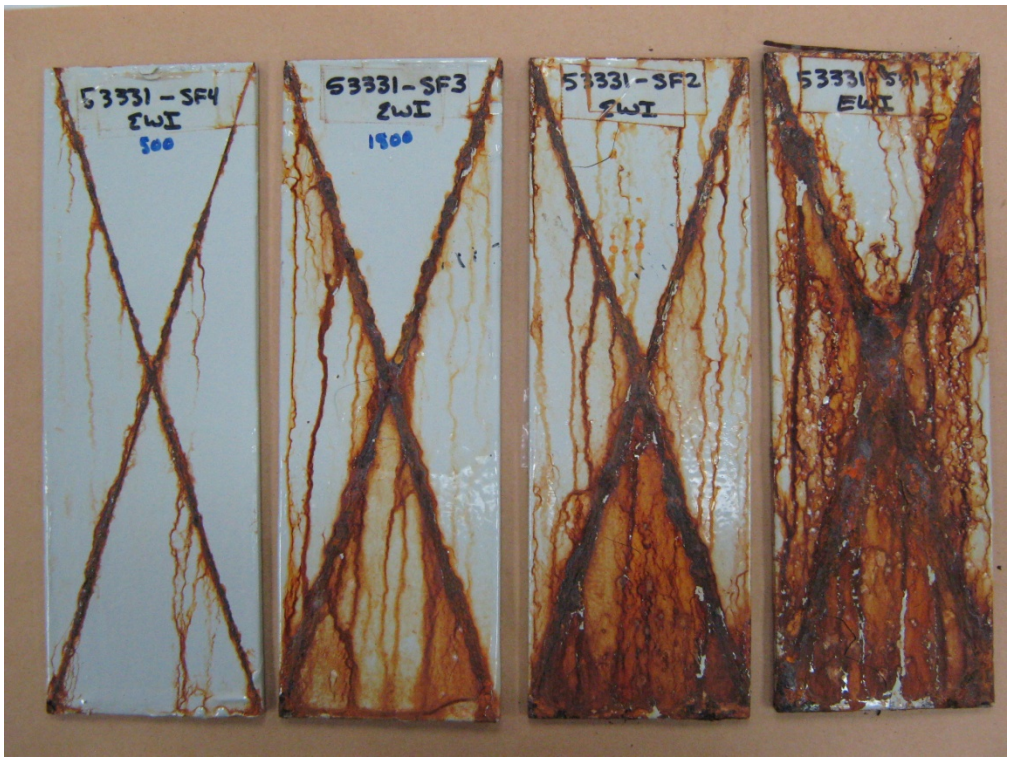

Figure B-4. EWI, Scribed to Metal. L→R: 500, 1500, 3000, 5000 Hours

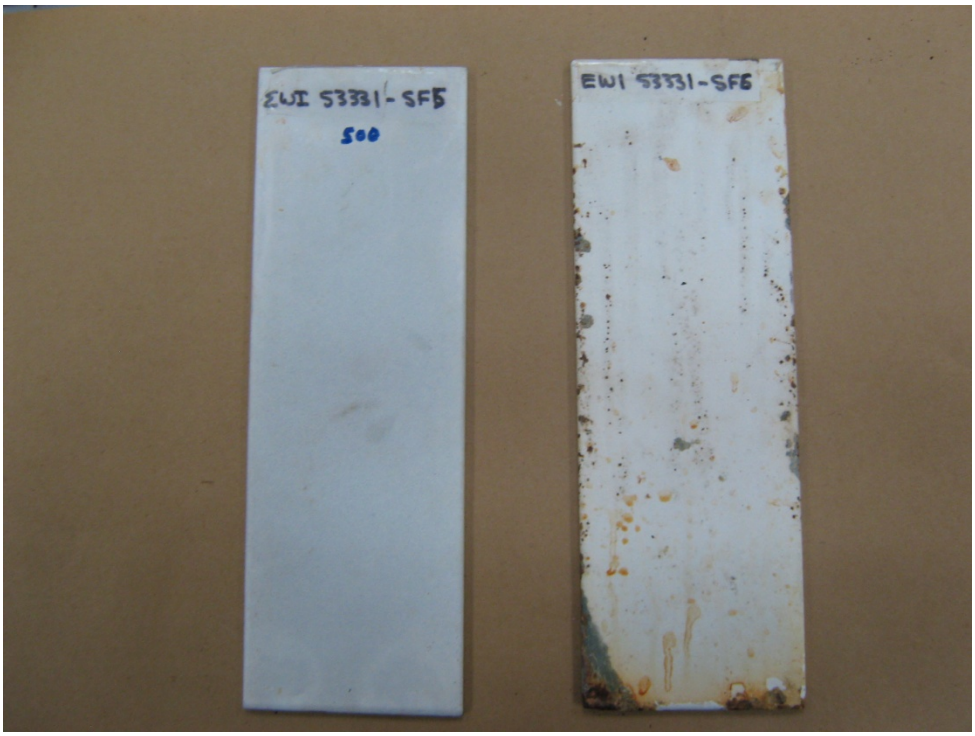

Figure B-5. EonCoat®, Back Side. L→R: 500, 1500 Hours

Abbreviations and Acronyms

ALL	EWI 3-step coating process, with post bake
ASTM	American Society for Testing and Materials
EC	EonCoat® ceramic coating
EDS	Elemental X-ray Dispersive Analysis
FAST	Facility for Accelerated Service Testing
FRA	Federal Railroad Administration
LIRR	Long Island Rail Road
PATH	Port Authority Trans-Hudson
PD	EWI 2-step coating process
PDZ	EWI 3-step coating process, without post bake
PZ	EWI 2-step process, not having the di-phenolic conversion, but with post bake
SEM	Scanning Electron Microscopy
TCRP/TTCI	Transit Cooperative Research Program/Transportation Technology Center, Inc.